

---

# Are Generative Classifiers More Robust to Adversarial Attacks?

---

Yingzhen Li<sup>1</sup> John Bradshaw<sup>1,2</sup> Yash Sharma<sup>3</sup>

## Abstract

There is a rising interest in studying the robustness of deep neural network classifiers against adversaries, with both advanced attack and defence techniques being actively developed. However, most recent work focuses on *discriminative* classifiers, which only model the conditional distribution of the labels given the inputs. In this paper we propose the *deep Bayes* classifier, which improves classical naive Bayes with conditional deep generative models. We further develop detection methods for adversarial examples, which reject inputs that have negative log-likelihood under the generative model exceeding a threshold pre-specified using training data. Experimental results suggest that deep Bayes classifiers are more robust than deep discriminative classifiers, and the proposed detection methods achieve high detection rates against many recently proposed attacks.

## 1. Introduction

Deep neural networks have been shown to be vulnerable to adversarial examples (Szegedy et al., 2013; Goodfellow et al., 2014). The latest attack techniques can easily fool a deep neural network with imperceptible perturbations (Goodfellow et al., 2014; Papernot et al., 2016b; Carlini & Wagner, 2017a; Kurakin et al., 2016; Madry et al., 2018; Chen et al., 2017a). These adversarial examples can also be generated in the black-box case, only requiring the ability to query the victim classifier (Papernot et al., 2017b; Chen et al., 2017b; Alzantot et al., 2018a). Adversarial attacks are a serious security threat to machine learning systems, threatening applications beyond image classification (Carlini & Wagner, 2018; Alzantot et al., 2018b).

To address this outstanding security issue, researchers have proposed defence mechanisms against adversarial attacks.

---

<sup>1</sup>University of Cambridge, Cambridge, UK <sup>2</sup>Max Planck Institute for Intelligent Systems, Tübingen, Germany <sup>3</sup>Cooper Union, NY, USA. Correspondence to: Yingzhen Li <yl494@cam.ac.uk>.

Presented at the ICML 2018 workshop on Theoretical Foundations and Applications of Deep Generative Models. Copyright 2018 by the author(s).

Adversarial training, which augments the training data with adversarially perturbed inputs, has shown moderate success at defending against recently proposed attack techniques (Szegedy et al., 2013; Goodfellow et al., 2014; Tramèr et al., 2017; Madry et al., 2018). In addition, recent advances in Bayesian neural networks have demonstrated that uncertainty estimates can be used to detect adversarial attacks (Li & Gal, 2017; Feinman et al., 2017; Louizos & Welling, 2017). Another notable category of defence techniques involves the usage of generative models. For example, Gu & Rigazio (2014) used an auto-encoder to denoise the inputs before feeding them to the classifier. This denoising approach has been extensively investigated, and the “denoisers” in usage include generative adversarial networks (Samangouei et al., 2018), PixelCNNs (Song et al., 2018) and denoising auto-encoders (Kurakin et al., 2018). These developments rely on the “off-manifold” conjecture, that is, that adversarial examples are far away from the data manifold, although Gilmer et al. (2018) has challenged this observation with a synthetic example.

Surprisingly, much less recent work has investigated the robustness of *generative classifiers* (Ng & Jordan, 2002) against adversarial attacks for multi-class classification, where such classifiers explicitly model the conditional distribution of the inputs given labels. Typically, a generative classifier produces predictions by comparing between the likelihood of the labels for a given input, which is closely related to the “distance” of the input to the data manifold associated with a class. Therefore, generative classifiers should be robust to proposed adversarial attacks if the “off-manifold” conjecture holds for many real-world applications. Unfortunately, many generative classifiers in popular use, including naive Bayes and linear discriminant analysis (Fisher, 1936), perform poorly on natural image classification tasks, making it difficult to verify the “off-manifold” conjecture with these tools.

Are generative classifiers more robust to recently proposed adversarial attack techniques? To answer this, we improve the naive Bayes algorithm by using conditional deep generative models, and evaluate the conjecture on the proposed generative classifier. In summary, our contributions include:

- We propose *deep Bayes* as an extension of the naive Bayes classifier, in which the conditional distribution

of an input given a label is parameterised by a deep latent variable model. We learn the latent variable model with the variational auto-encoder algorithm (Kingma & Welling, 2013; Rezende et al., 2014), and approximate Bayes’ rule using importance sampling.

- We propose three detection methods for adversarial perturbations. The first two use the learned generative model as a proxy of the data manifold, and reject inputs that are far away from it. The third computes statistics for the classifier’s output probability vector on training data, and rejects inputs that lead to under- and over-confident predictions.
- We evaluate the robustness of the proposed generative classifier on the MNIST multi-class and CIFAR binary classification tasks. We also compare the generative classifiers with a number of discriminative classifiers including Bayesian neural networks and *discriminative* latent variable models.

## 2. Deep Bayes: conditional latent variable model as a generative classifier

Denote  $p_{\mathcal{D}}(\mathbf{x}, \mathbf{y})$  the data distribution for the input  $\mathbf{x} \in \mathbb{R}^D$  and label  $\mathbf{y} \in \{\mathbf{y}_c | c = 1, \dots, C\}$ , where  $\mathbf{y}_c$  denotes the one-hot encoding vector for class  $c$ . For a given  $\mathbf{x} \in \mathbb{R}^D$  we can define the ground-truth label by

$$\mathbf{y} \sim p_{\mathcal{D}}(\mathbf{y}|\mathbf{x}) \quad \text{if } \mathbf{x} \in \text{supp}(p_{\mathcal{D}}(\mathbf{x})). \quad (1)$$

Importantly we do not assume a ground-truth label for  $\mathbf{x} \notin \text{supp}(p_{\mathcal{D}}(\mathbf{x}))$ . We assume that the data distribution  $p_{\mathcal{D}}(\mathbf{x}, \mathbf{y})$  follows the *manifold assumption*, i.e. for every class  $c$ , the corresponding conditional distribution  $p_{\mathcal{D}}(\mathbf{x}|\mathbf{y}_c)$  has its support as a low-dimensional manifold  $\mathcal{M}_c = \text{supp}(p_{\mathcal{D}}(\mathbf{x}|\mathbf{y}_c))$ . Therefore the training dataset  $\mathcal{D} = \{(\mathbf{x}^{(n)}, \mathbf{y}^{(n)})\}_{n=1}^N$  is generated as the following:

$$(\mathbf{x}^{(n)}, \mathbf{y}^{(n)}) \sim p_{\mathcal{D}}(\mathbf{x}, \mathbf{y}) \Leftrightarrow \mathbf{y}^{(n)} \sim p_{\mathcal{D}}(\mathbf{y}), \mathbf{x}^{(n)} \sim p_{\mathcal{D}}(\mathbf{x}|\mathbf{y}).$$

We denote  $\hat{p}_{\mathcal{D}}$  as the training data empirical distribution of  $p_{\mathcal{D}}$  and assume a balanced data setting, i.e.  $\hat{p}_{\mathcal{D}}(\mathbf{y}) = p_{\mathcal{D}}(\mathbf{y}) = \text{Uniform}(\mathbf{y})$ .

A (Bayesian) generative classifier first builds a *conditional generative model*  $p(\mathbf{x}, \mathbf{y}) = p(\mathbf{x}|\mathbf{y})p(\mathbf{y})$ , often with  $p(\mathbf{y}) = p_{\mathcal{D}}(\mathbf{y})$ , and then, in prediction time, predicts the label  $\mathbf{y}^*$  of a test input  $\mathbf{x}^*$  using Bayes’ rule,

$$p(\mathbf{y}^*|\mathbf{x}^*) = \frac{p(\mathbf{x}^*|\mathbf{y}^*)p(\mathbf{y}^*)}{p(\mathbf{x}^*)} = \text{softmax}_{c=1}^C [\log p(\mathbf{x}^*, \mathbf{y}_c)],$$

where  $\text{softmax}_{c=1}^C$  denotes the softmax operator over the  $c$  axis. Therefore, the output probability vector is computed analogously to many deep discriminative classifiers which use softmax activation in the output layer, so many

existing attacks can be tested directly. However, unlike discriminative classifiers, the “logit” values prior to softmax activation have a clear meaning in deep Bayes classifiers, the (approximated) test log-likelihood  $\log p(\mathbf{x}^*|\mathbf{y}_c)$  of input  $\mathbf{x}^*$  conditioned on a given label  $\mathbf{y}_c$ . Therefore, one can also analyse the logit values to determine whether the unseen input  $\mathbf{x}^*$  is legitimate, a utility which will be discussed further in later sections.

*Naive Bayes* is perhaps the most well-known generative classifier; it assumes a factorised distribution for the conditional generator, i.e.  $p(\mathbf{x}|\mathbf{y}) = \prod_{d=1}^D p(x_d|\mathbf{y})$ . However naive Bayes is less suitable for e.g. image and speech data, where the factorisation assumption is inappropriate. Fortunately, we can leverage the recent advances in generative modelling and apply a deep generative model for the joint distribution  $p(\mathbf{x}, \mathbf{y})$ . We refer to such generative classifiers that use deep generative models as *deep Bayes* classifiers.

When a deep latent variable model (LVM)  $p(\mathbf{x}, \mathbf{z}, \mathbf{y})$  is in use, the conditional distribution is  $p(\mathbf{x}|\mathbf{y}) = \frac{\int p(\mathbf{x}, \mathbf{z}, \mathbf{y}) d\mathbf{z}}{\int p(\mathbf{x}, \mathbf{z}, \mathbf{y}) d\mathbf{z} d\mathbf{x}}$ . Importantly, this leads to a conditional distribution  $p(\mathbf{x}|\mathbf{y})$  that is *not* factorised, which is much more powerful than naive Bayes. Since maximum likelihood is intractable, we follow Kingma & Welling (2013); Rezende et al. (2014) to introduce an amortised approximate posterior  $q(\mathbf{z}|\mathbf{x}, \mathbf{y})$ , and train both the generative model  $p$  and the inference network  $q$  by maximising the variational lower-bound:

$$\mathbb{E}_{\mathcal{D}}[\mathcal{L}_{\text{VI}}(\mathbf{x}, \mathbf{y})] = \frac{1}{N} \sum_{n=1}^N \mathbb{E}_q \left[ \log \frac{p(\mathbf{x}_n, \mathbf{z}_n, \mathbf{y}_n)}{q(\mathbf{z}_n|\mathbf{x}_n, \mathbf{y}_n)} \right]. \quad (2)$$

After training, the predicted class probability vector  $\mathbf{y}^*$  for a future input  $\mathbf{x}^*$  is (approximately) computed by Bayes’ rule with Monte Carlo samples  $\mathbf{z}_c^k \sim q(\mathbf{z}|\mathbf{x}^*, \mathbf{y}_c)$ :

$$p(\mathbf{y}^*|\mathbf{x}^*) \approx \text{softmax}_{c=1}^C \left[ \log \sum_{k=1}^K \frac{p(\mathbf{x}^*, \mathbf{z}_c^k, \mathbf{y}_c)}{q(\mathbf{z}_c^k|\mathbf{x}^*, \mathbf{y}_c)} \right]. \quad (3)$$

We evaluate the effect of the following factorisation structures on the robustness of the generative model  $p(\mathbf{x}, \mathbf{z}, \mathbf{y})$  (see Figure 1).

$$p(\mathbf{x}, \mathbf{z}, \mathbf{y}) = p(\mathbf{z})p(\mathbf{y}|\mathbf{z})p(\mathbf{x}|\mathbf{z}, \mathbf{y}) \quad (\text{GFZ})$$

$$p(\mathbf{x}, \mathbf{z}, \mathbf{y}) = p_{\mathcal{D}}(\mathbf{y})p(\mathbf{z}|\mathbf{y})p(\mathbf{x}|\mathbf{z}, \mathbf{y}) \quad (\text{GFY})$$

$$p(\mathbf{x}, \mathbf{z}, \mathbf{y}) = p_{\mathcal{D}}(\mathbf{x})p(\mathbf{z}|\mathbf{x})p(\mathbf{y}|\mathbf{z}, \mathbf{x}) \quad (\text{DFX})$$

$$p(\mathbf{x}, \mathbf{z}, \mathbf{y}) = p(\mathbf{z})p(\mathbf{y}|\mathbf{z})p(\mathbf{x}|\mathbf{z}) \quad (\text{GBZ})$$

$$p(\mathbf{x}, \mathbf{z}, \mathbf{y}) = p_{\mathcal{D}}(\mathbf{y})p(\mathbf{z}|\mathbf{y})p(\mathbf{x}|\mathbf{z}) \quad (\text{GBY})$$

$$p(\mathbf{x}, \mathbf{z}, \mathbf{y}) = p_{\mathcal{D}}(\mathbf{x})p(\mathbf{z}|\mathbf{x})p(\mathbf{y}|\mathbf{z}) \quad (\text{DBX})$$

$$p(\mathbf{x}, \mathbf{z}, \mathbf{y}) = p(\mathbf{z})p(\mathbf{x}|\mathbf{z})p(\mathbf{y}|\mathbf{z}, \mathbf{x}) \quad (\text{DFZ})$$

We use the initial character “G” to denote generative classifiers and “D” to denote discriminative classifiers. Models

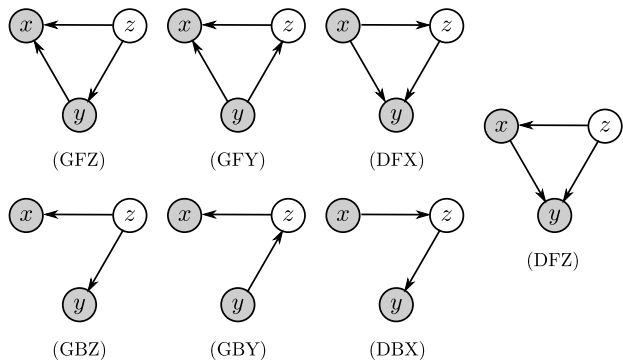


Figure 1. A visualisation of the graphical models, including both Generative and Discriminative ones, as well as Fully connected and Bottleneck ones. The last character indicates the first node in the topological order of the graph.

with the second character as “F” have a *fully connected* graph, while “B” models do not have direct connection between  $x$  and  $y$ , thus enforcing the usage of the latent code  $z$  as a *bottleneck*. The last character of the model name indicates the first node in topological order. Model DFZ is somewhat intermediate, as it builds a generative model for the inputs  $x$  but also directly parameterises the conditional distribution  $p(y|x, z)$ . We do not test other model combinations under this nomenclature, as either the graph contains directed cycles (e.g.  $x \rightarrow y \rightarrow z \rightarrow x$ ), or  $z$  is the last node in topological order (e.g.  $x \rightarrow y, (x, y) \rightarrow z$ ) so that the marginalisation of  $z$  does not affect classification.

### 3. Detecting adversarial attacks with generative classifiers

We propose detection methods for adversarial examples using deep generative models. As an illustrating example, consider a labelled dataset of “cat” and “dog” images. If an adversarial image of a cat  $x_{adv}$  is incorrectly labelled as “dog”, then either this image is ambiguous, or, under a *perfect* generative model, the logit  $\log p(x_{adv}, \text{“dog”})$  will be significantly lower than normal. This means we can detect attacks using the logits  $\log p(x^*, y_c), c = 1, \dots, C$  computed on a test input  $x^*$  by comparing them with the logits computed on legitimate training inputs.

Concretely, the proposed detection algorithms are as follows. Our proposals aim to reject both unlabelled input  $x$  that has low probability under  $p_D(x)$ , and labelled data  $(x, y)$  that has low probability under  $p_D(x, y)$ .

- **Marginal detection:** rejecting inputs that are far away from the manifold.  
One can select a threshold  $\delta$  and reject an input  $x$  if  $-\log p(x) > \delta$ . To determine the threshold  $\delta$ , we can compute  $\bar{d}_D = \mathbb{E}_{x \sim \mathcal{D}}[-\log p(x)]$  and  $\sigma_D =$

$\sqrt{\mathbb{V}_{x \sim \mathcal{D}}[\log p(x)]}$ , then set  $\delta = \bar{d}_D + \alpha \sigma_D$ . It is also possible to compute the statistics  $\bar{d}_p, \sigma_p$  on the images generated by the generative model accordingly.

- **Logit detection:** rejecting inputs using joint density.  
Given a victim model  $y = F(x)$ , one can reject  $x$  if  $-\log p(x, F(x)) > \delta$ . For generative classifiers, one can use the mean and variance statistics  $\bar{d}_c, \sigma_c$  computed on  $\log p(x|y_c)$  and select  $\delta = \bar{d}_c + \alpha \sigma_c$ .
- **KL detection:** rejecting inputs with over- and/or under-confident predictions.  
Denote  $p(x)$  as a  $C$ -dimensional probability vector outputted by the classifier. For each class  $c$ , we first collect the *mean classification probability vector*  $p_c = \text{mean}\{p(x) | (x, y_c) \in \mathcal{D}\}$ , then compute the mean  $\bar{d}_c$  and standard deviation  $\sigma_c$  on the KL divergence  $\text{KL}[p_c || p(x)]$  for all  $(x, y_c) \in \mathcal{D}$ . Then, a test input  $x^*$  with prediction label  $c^* = \arg \max p(x^*)$  is rejected if  $\text{KL}[p_{c^*} || p(x^*)] > \bar{d}_{c^*} + \alpha \sigma_{c^*}$ . Therefore, an example  $x^*$  will be rejected if the classifier is over-confident or under-confident (far away from data manifold or ambiguous inputs).

We emphasise that a powerful generative model is required for this detection task since the data distribution  $p_D(x, y)$  is approximated by  $p(x, y)$ . Otherwise a poor generative model paired with the above detection methods can reject many legitimate inputs. Note that detection methods based on modelling logit values and/or denoising methods have also been considered in the literature (e.g. Li & Gal, 2017; Feinman et al., 2017; Song et al., 2018). But, as the logit values in deep Bayes represent the probability of generating the input  $x$  given the class label  $y = y_c$ , we can use the marginal and logit detection methods to directly verify the “off-manifold” adversarial example conjecture.

### 4. Experiments

We carry out a number of tests on the proposed deep Bayes classifiers (3), where  $q(z|\cdot)$  and  $p(z|\cdot)$  are factorised Gaussians, and the conditional probability  $p(x|\cdot)$ , if required, is parameterised by an  $\ell_2$  loss. Besides the LVM-based classifiers, we further train a Bayesian neural network (BNN) with Bernoulli dropout (dropout rate 0.3), as it has been shown in Li & Gal (2017); Feinman et al. (2017) that BNNs are more robust than their deterministic counterparts. The constructed BNN has 2x more channels than LVM-based classifiers, making the comparison slightly “unfair”, as the BNN layers have more capacity. We use  $K = 10$  Monte Carlo samples for all the classifiers.

The adversarial attacks in test include both  $\ell_\infty$  and  $\ell_2$  untargeted attacks: fast gradient sign method (FGSM, Goodfellow et al., 2014), projected gradient descent (PGD, Madry et al., 2018), momentum iterative attack (MIM, Dong et al.,

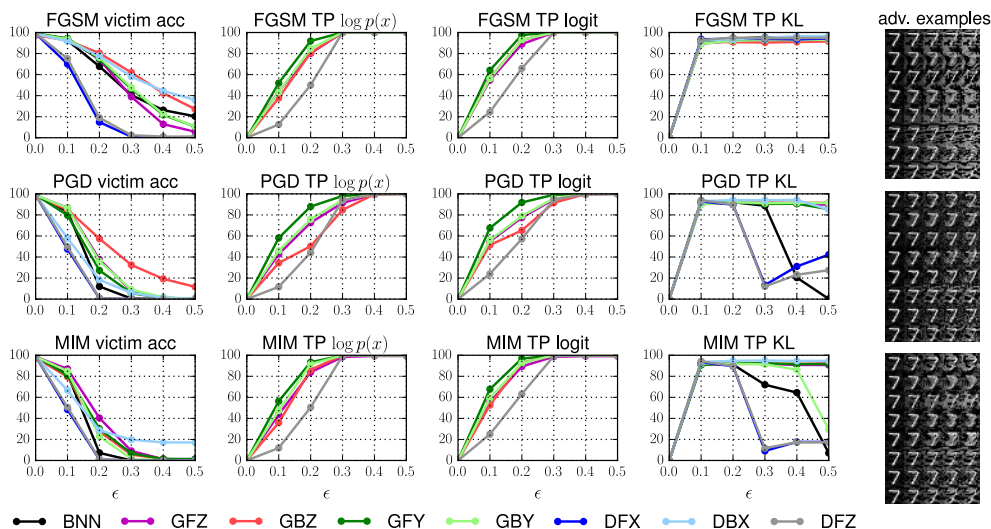


Figure 2. Accuracies (column 1) and detection rates (columns 2-4) against **white-box**  $\ell_\infty$  attacks on MNIST. The higher the better. The right most column visualises crafted adversarial examples on an image of digit “7”, with  $\ell_\infty$  distortion  $\epsilon$  growing from 0.1 to 0.5.

2017) and Carlini & Wagner  $\ell_2$  (CW, Carlini & Wagner, 2017a). All the attacks are taken from the CleverHans 2.0 library (Papernot et al., 2017a). Two metrics are reported: *accuracy* of the classifier on crafted adversarial examples, and *detection rate* of the classifier on adversarial examples that have successfully fooled the classifier to predict wrong labels. This detection rate is defined as the true positive (TP) rate of finding an adversarial example, and the detection threshold is selected to achieve a 5% false positive rate on clean data. Due to page limit, we only visualise the performances in the main text. Readers are referred to the appendix for results in tables as well as further experiments.

#### 4.1. MNIST

The first set of experiments evaluate the robustness of generative classifiers on MNIST. Here the image pixel values are normalised to  $[0, 1]$ , and the LVM-based classifiers have  $\dim(z) = 64$ .

**White-box attacks ( $\ell_\infty$ )** We first perform white-box attacks, i.e. the attacker can differentiate through the classifier to craft adversarial examples. Results for  $\ell_\infty$  attacks are reported in Figure 2. Although FGSM is a weak attack, DFX & DFZ are not robust to it even when  $\epsilon = 0.2$  (where the adversarial examples are still visually close to the original digit “7”). Other classifiers perform better. PGD & MIM, as stronger attacks, achieve better success rates on all classifiers, but the generative classifiers with bottleneck perform generally better than the discriminative ones. Interestingly, DBX is the most robust against FGSM & MIM, which agrees with the preliminary tests in Alemi et al. (2017). But, this model is less robust to PGD, in this case GBZ is a clear winner. This demonstrates that the usage of bottleneck is beneficial for better robustness of MNIST classifiers.

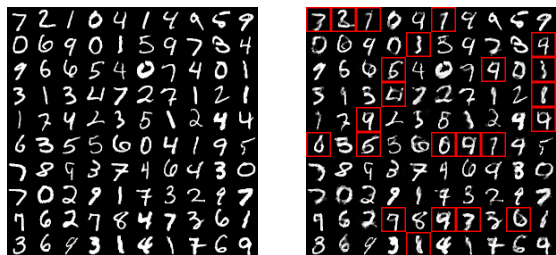
In terms of detection, generative classifiers have successfully detected the adversarial examples with  $\epsilon \geq 0.3$ , which is reasonable as the visual distortion is already significant. Importantly, for the generative classifiers, we observe that robustness decreases as the  $\ell_\infty$  distortion  $\epsilon$  increases, but at the same time the TP rates for marginal and logit detection also increase. This clearly demonstrates that these three  $\ell_\infty$  attacks are ineffective for generative classifiers, as they fail to find near-manifold adversarial examples that fool both the classifier and the detection methods. DFZ as an intermediate between generative and discriminative classifiers has worse robustness results (also worse detection with KL), but has good detection performance for the marginal and logit metrics. This is because with softmax activation, the marginal distribution  $p(x)$  is dropped, but in marginal/logit detection  $p(x)$  is still in use.

**White-box attack ( $\ell_2$ )** For the CW  $\ell_2$  attack, we performed a hyper-parameter search for the loss-balancing parameter  $c$  ( $\ell_2$  distortion increases with larger  $c$ ) in  $\{0.1, 1.0, 10.0, 100.0, 1000.0\}$  on the first 100 test images, and we found  $c = 10.0$  returns the highest success rate. Victim accuracy and detection rates are reported in Table 1, and we see that CW, though successful in terms of fooling many classifiers to predict wrongly, failed on attacking GBZ. Also, the  $\ell_2$  distortions of the successful attacks on generative classifiers are significantly larger. Furthermore, we found the success of the attack on GFZ & GFY is mainly due to the ambiguity of the crafted adversarial images. As visualised in Figure 3, the induced distortion from CW leads to ambiguous digits, significant ambiguity is denoted by the red rectangles. In the appendix, we visualize the adversarial examples generated on all classifiers, showing that the CW adversarial examples crafted on generative classifiers are

## Are Generative Classifiers More Robust to Adversarial Attacks?

Table 1. CW- $\ell_2$  attack results ( $c = 10.0$ ). Here, accuracy (adv) measures classifying the adversarial inputs to the original classes.

	acc. (clean)	acc. (adv)	$\ell_2$ dist.	TP KL
BNN	99.12%	24.40%	2.129	95.31
GFZ	98.55%	28.58%	2.663	95.37
GBZ	97.45%	81.51%	2.446	91.01
GFY	99.15%	28.64%	2.732	96.03
GBY	98.72%	32.72%	2.735	94.46
DFX	99.10%	20.31%	2.095	99.96
DBX	98.87%	30.19%	1.806	96.76
DFZ	99.10%	13.60%	2.188	99.57



(a) clean inputs (b) CW adv. inputs (GFZ)

Figure 3. Visualising the clean inputs and the crafted adversarial examples. GFY results are similar to GFZ, and the digits in the red rectangles show significant ambiguity.

more ambiguous than those crafted on discriminative ones. With the KL detection method, all classifiers achieve  $> 95\%$  detection rates, which is as expected as the default CW attack configuration, by construction, generates adversarial examples that lead to minimal difference between the logit values of the most and the second most probable labels.

**Grey-box attacks** Athalye et al. (2018) claimed that if a successful defence against white-box attacks is due to gradient masking, then this defence is likely to be less effective against grey-box/black-box attacks, as they do not differentiate through the victim classifier and the defence mechanism (Papernot et al., 2017b). Therefore, we consider a grey-box setting where the attacker has access to the output probability vectors of the classifiers on the training data. We distill a victim classifier using a “student” CNN to achieve  $> 99\%$  agreement on test data. Then, the adversarial examples are crafted on the substitute model. We report three metrics: the accuracy of the substitute CNN on the crafted examples (to ensure the crafted examples fool the substitute), the accuracy of the victim classifier on the crafted examples (to test transferability), and the detection rate defined as before.

We visualise the metrics in Figure 4. For PGD and MIM, the substitute models’ accuracies are on par with the white-box victim accuracies for  $\epsilon = 0.1$ , but eventually the adversary fools the substitutes with increased  $\epsilon$ . However, analyzing the victim accuracies, we see that grey-box attacks do not transfer very well, especially for the generative classifiers, where the victim accuracies are still around

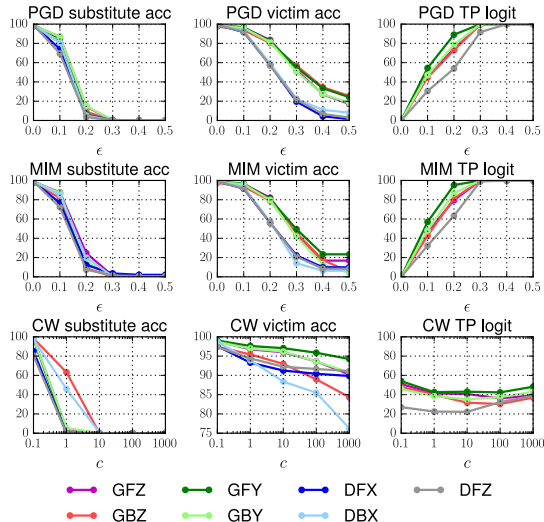


Figure 4. Accuracy and detection rates against grey-box attacks on MNIST. The higher the better.

50%  $\sim$  60% when  $\epsilon = 0.3$  (c.f. white-box victim accuracy  $< 10\%$  for PGD). Also, the detection rates are around 100% for  $\epsilon = 0.3$ , meaning that most of the grey-box adversarial images are also off the data manifold. The CW attack with a decently large  $c$  value is very effective on the substitute models, but still the generated adversarial examples fail to transfer, and classifier GFY achieves the best accuracy against them. Interestingly, the bottleneck classifiers are generally less robust to the grey-box CW attack when compared to their fully-connected counterparts.

**Black-box attacks** We additionally evaluate a black-box attack that only assumes access to queried labels. In other words, the attacker has no knowledge about the training data nor the victim model, they can only query the victim classifier for the labels on given inputs. We follow Papernot et al. (2017b) to train a substitute CNN using Jacobian-based dataset augmentation. Assume  $F(x)$  is the probability vector output of the substitute model, then at the  $t^{\text{th}}$  outer-loop, we train  $F$  on dataset  $\mathcal{D}_t = \{(x_n, y_n)\}$  with queried  $y_n$  for 10 epochs, and augment the dataset by

$$\mathcal{D}_{t+1} = \mathcal{D}_t \cup \{\mathbf{x} + \lambda \nabla_{\mathbf{x}} F(\mathbf{x})^T \mathbf{y} \mid (\mathbf{x}, \mathbf{y}) \in \mathcal{D}_t\}. \quad (4)$$

We initialise  $\mathcal{D}_1$  with  $200 \times 10$  datapoints from the MNIST test set, select  $\lambda = 0.1$ , and run the algorithm for 6 outer-loops. This results in 64,000 queried inputs and  $\sim 96\%$  accuracy of the substitute model on test data. The results are visualised in Figure 5, similarly we see that the black-box attack of Papernot et al. (2017b) is ineffective on generative classifiers. Interestingly, the generative bottleneck classifiers GBZ and GBY seem to be slightly more robust to black-box PGD & MIM attacks, and for the discriminative classifiers, the robustness results against CW are slightly improved when compared to the grey-box cases.

## Are Generative Classifiers More Robust to Adversarial Attacks?

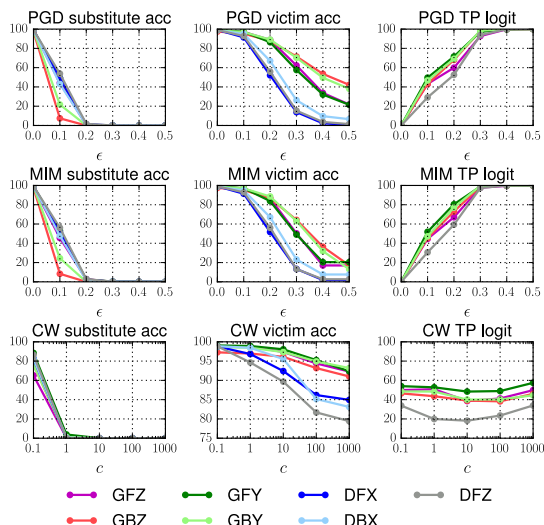


Figure 5. Accuracy and detection rates against **black-box** attacks on MNIST. The higher the better.

**Cross-model attack transferability** Finally, we report in Figure 6 the transferability results of the crafted adversarial examples between different models (Papernot et al., 2016a). Here we take adversarial examples crafted in the white-box setting with PGD and MIM ( $\epsilon = 0.3$ ), and transfer successful ones to other classifiers. The transfer is effective between generative classifiers but not from generative to discriminative (and vice versa). Especially the attacks crafted on **DBX** do not transfer in general, at the same time, **DFX** is the least robust model in this case. Furthermore, the generative classifiers obtain very high detection rates on all transferred attacks ( $> 95\%$ ). This again demonstrates that the generative classifiers are more robust against this transferred attack across different models.

### 4.2. CIFAR (binary)

In this section we consider the same set of evaluations on CIFAR-10 data containing natural images. Unfortunately, we failed to obtain generative classifiers with comparable test accuracies to discriminative deep neural networks: the clean accuracies for **GFZ** & **GFY** are all  $< 50\%$ . Even when using the conditional PixelCNN++ (Salimans et al., 2017) (which uses much deeper networks), the clean accuracy on the test data is 72.40%, while a CNN can easily get  $> 80\%$  test accuracy. Therefore, we consider a simpler binary classification problem and construct a dataset containing CIFAR images from the “airplane” and “frog” categories. The images in this dataset are scaled to  $[0, 1]$ . On this dataset, the generative classifiers use  $\dim(z) = 128$  and obtain  $> 90\%$  clean test accuracy, with the exact numbers reported in the appendix. The attacks are performed on the test images that all models initially correctly classify, leading to a test set of 1577 instances.

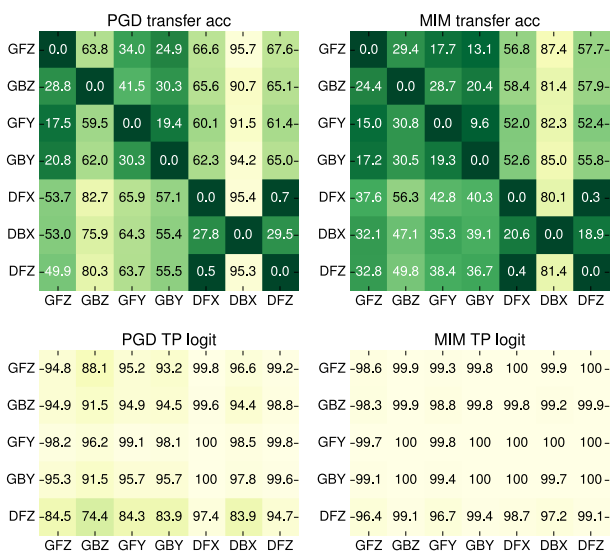


Figure 6. Accuracy and detection rates against **cross-model transfer** attacks on MNIST. The horizontal axis corresponds to the source victim that the adversarial examples are crafted on, and the vertical axis corresponds to the target victim that the attacks are transferred to. The higher (i.e. the lighter) the better.

**White-box attacks ( $\ell_\infty$ )** We present the white-box  $\ell_\infty$  attack results in Figure 7, where the distortion strengths are selected as  $\epsilon \in \{0.01, 0.02, 0.05, 0.1, 0.2\}$ . Again, generative classifiers are more robust than the discriminative ones, but **GBZ** is the most robust, much better than the others when  $\epsilon \geq 0.05$ . BNN is significantly better than other discriminative VAE-based classifiers, presumably due to higher randomness. However, the detection rates with marginal probability and logit values are less satisfactory, as the methods fail to detect attacks with  $\epsilon = 0.1$  (which attain both high success rate and visually perceptible distortion). KL detection performs much better, and interestingly, discriminative classifiers dominate in this metric. These detection results suggest that the  $\ell_2$  likelihood might not be best suited for modelling natural images, which has also been suggested in prior work (e.g. see Larsen et al., 2016; van den Oord et al., 2016). But, on the other hand, for generative classifiers the visual distortion of the PGD attacks is less significant than that of FGSM & MIM (especially when  $\epsilon = 0.2$ ), which also explains the lower TP rates for marginal and logit detection on PGD attacks.

**White-box attack ( $\ell_2$ )** As the test set is relatively small, we directly perform CW attacks on the test data with  $c \in \{0.1, 1, 10, 100, 1000\}$ . Results are visualised in Figure 8. The generative classifiers are significantly more robust than the other victim models (with the best being **GBZ**), and the  $\ell_2$  distortions computed on successful attacks are also significantly higher. The TP rates are low for marginal and logit detection, which is reasonable as the crafted im-

## Are Generative Classifiers More Robust to Adversarial Attacks?

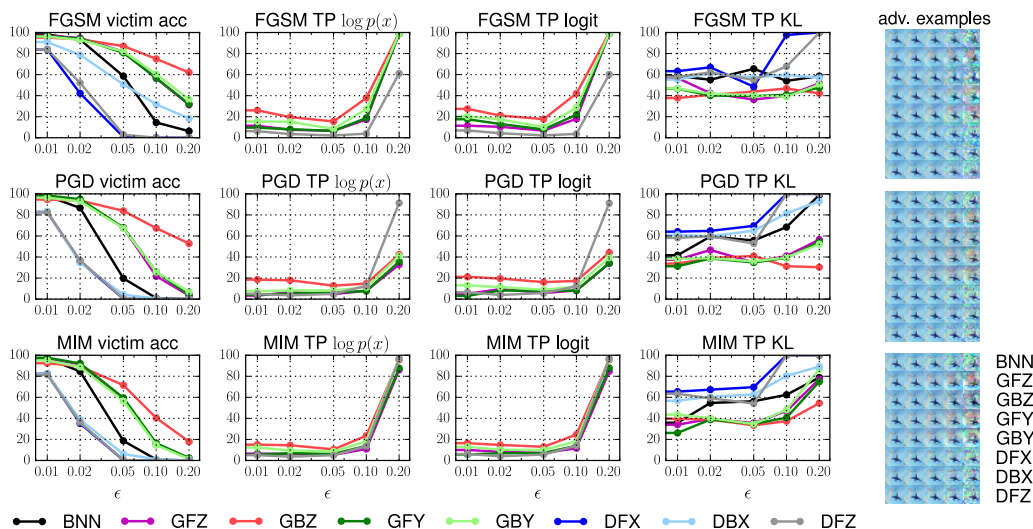


Figure 7. Accuracy and detection rates against **white-box**  $\ell_\infty$  attacks on the CIFAR plane-vs-frog dataset. The higher the better. The right most column visualises crafted adversarial examples on an image of a plane, with  $\ell_\infty$  distortion  $\epsilon \in \{0.01, 0.02, 0.05, 0.1, 0.2\}$ .

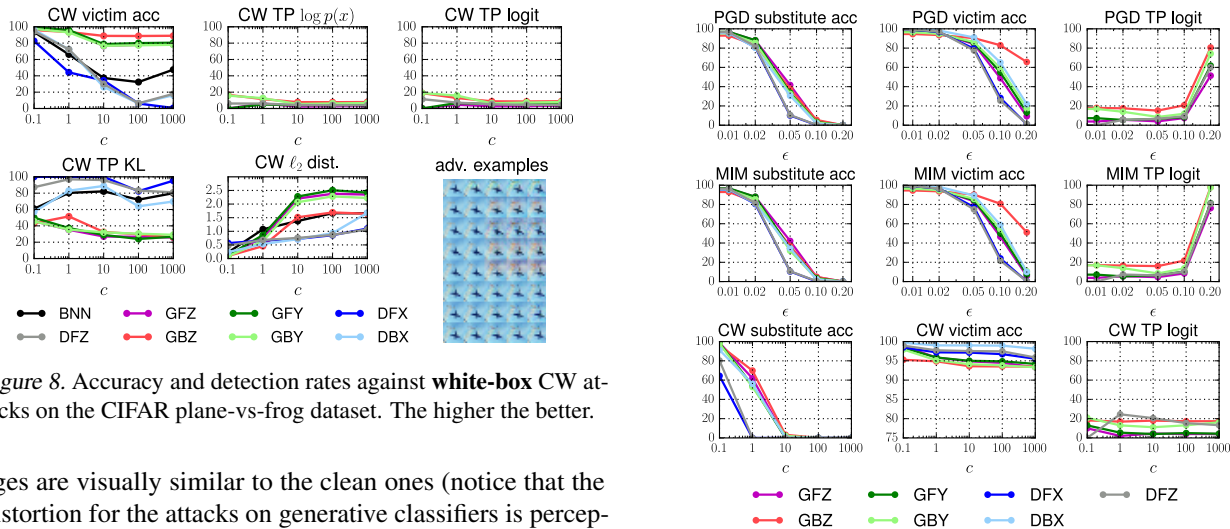


Figure 8. Accuracy and detection rates against **white-box** CW attacks on the CIFAR plane-vs-frog dataset. The higher the better.

ages are visually similar to the clean ones (notice that the distortion for the attacks on generative classifiers is perceptible). These results indicate that the CW white-box attack is ineffective when attacking generative classifiers.

**Grey-box attack** We perform our grey-box experiments with exactly the same setting as done with MNIST. Figure 9 shows that all the victim classifiers in test are robust to transferred attacks, with **GBZ** performing the best. Surprisingly, **DBX** is on par with other generative classifiers against PGD & MIM, and the discriminative classifiers are a bit most robust against grey-box CW. **DFX** performs the worst against the grey-box CW attack, although the difference is not significant. Again, the detection rates are low when the victim accuracies are high, indicating that grey-box attacks fail to generate near-manifold adversarial examples.

**Black-box attack** The setting is almost the same as done with MNIST, with the exception being that the initial query set  $\mathcal{D}_1$  contains  $200 \times 2$  datapoints (12,800 queries in to-

Figure 9. Accuracy and detection rates against **grey-box** attacks on the CIFAR plane-vs-frog dataset. The higher the better.

tal). The black-box substitutes achieve almost the same accuracy as their corresponding victim models on clean test datapoints. Figure 10 shows that the victim classifiers are robust to the PGD/MIM transferred attacks. Interestingly, **DBX** is slightly less robust to the black-box CW attack compared to in the grey-box case, but again the difference is not significant. In general, black-box CW attacks return high victim accuracies and low detection rates, meaning that the crafted examples are close to the data manifold.

**Cross-model attack transferability** Finally, we present the CIFAR cross-model attack transferability results in Figure 11, and here we select  $\epsilon = 0.1$  instead. Again, transferred attacks are less effective across the victim models. However, the TP rates for logit are significantly

## Are Generative Classifiers More Robust to Adversarial Attacks?

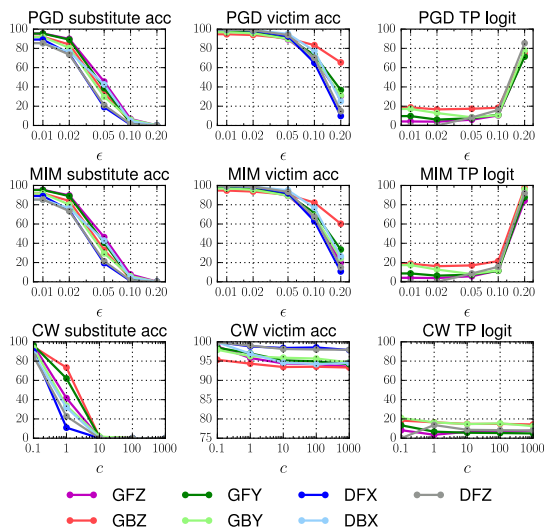


Figure 10. Accuracy and detection rates against **black-box** attacks on the CIFAR plane-vs-frog dataset. The higher the better.

lower than in the MNIST case (also see Figure 7). Nevertheless, the detection rates for the “discriminative to generative” transfer are considerably higher. Combined with the accuracy results, we see that discriminative models as substitutes are ineffective in the transferred attack setting.

### 5. Discussion

We have presented initial evidence that generative classifiers are more robust to recently proposed adversarial attacks than discriminative classifiers. Many existing attacks require significantly larger distortions in order to fool the deep Bayes classifier, and at the same time, this increased distortion makes the adversarial images less likely to evade generative model-based detection methods. Our experiments show that modelling unobserved variables is effective for defending against adversarial attacks, which agrees with the Bayesian neural network literature (Li & Gal, 2017; Feinman et al., 2017; Carlini & Wagner, 2017b).<sup>1</sup> But more importantly, the structure of the graphical model has significant impact on robustness, and we show that deep latent variable model-based generative classifiers generally outperform the (randomised) discriminative ones. As an aside, k-nearest neighbours as another type of generative classifier has also been shown to be robust if deep feature representations are leveraged (Papernot & McDaniel, 2018).

While we have given preliminary evidence to suggest that generative classifiers are more robust to current adversarial attacks, we do not wish to claim that these models will be robust to *all* possible attacks. Aside from many recent attacks being designed specifically for discriminative neural net-

<sup>1</sup>In Bayesian neural networks, the network weights are treated as unobserved/latent variables.

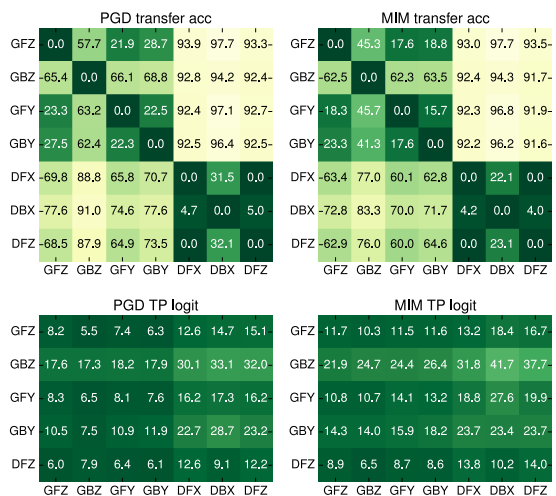


Figure 11. Accuracy and detection rates against **cross-model transfer** attacks on the CIFAR plane-vs-frog dataset. The horizontal axis corresponds to the source victim, and the vertical axis corresponds to the target victim. The higher (lighter) the better.

works, there is also evidence for the fragility of generative models; e.g. naive Bayes as a standard approach for spam filtering is well-known to be fragile (Dalvi et al., 2004; Huang et al., 2011), and very recently Tabacof et al. (2016); Kos et al. (2017); Creswell et al. (2017) also designed attacks for (unconditional) VAE-type models. However, generative classifiers can be made more robust too, to counter these weaknesses. Dalvi et al. (2004) have shown that generative classifiers can be made more secure if aware of the attack strategy, and Biggio et al. (2011; 2014) further improved naive Bayes’ robustness by modelling the conditional distribution of the adversarial inputs. These approaches are similar to the adversarial training of discriminative classifiers, and efficient ways for doing so with generative classifiers can be an interesting research direction.

We are aware of the argument of Carlini & Wagner (2017b), that MNIST properties might not hold on natural images, and we account for that by testing the robustness of deep Bayes on a binary classification task derived from CIFAR-10. Future work will verify the robustness of generative classifiers on the full CIFAR-10 dataset and beyond, but as mentioned, existing deep generative models are less suited for this purpose. Indeed, PixelCNN-based classifiers perform relatively poorly on CIFAR-10, and in general, generative classifiers are less accurate than discriminative classifiers at classifying legitimate inputs (Efron, 1975; Ng & Jordan, 2002). Also, they are much more computationally expensive, limiting their current application to large-scale datasets such as ImageNet. Therefore, it still remains a research challenge to verify the robustness conjecture on natural images in the wild. We believe that progress on this topic can inspire better designs of attack, defence and detection techniques with generative models.



## References

- Alemi, A. A., Fischer, I., Dillon, J. V., and Murphy, K. Deep variational information bottleneck. In *International Conference on Learning Representations*, 2017.
- Alzantot, M., Sharma, Y., Chakraborty, S., and Srivastava, M. Genattack: Practical black-box attacks with gradient-free optimization. *arXiv preprint arXiv:1805.11090*, 2018a.
- Alzantot, M., Sharma, Y., Elgohary, A., Ho, B.-J., Srivastava, M., and Chang, K.-W. Generating natural language adversarial examples. *arXiv preprint arXiv:1804.07998*, 2018b.
- Athalye, A., Carlini, N., and Wagner, D. Obfuscated gradients give a false sense of security: Circumventing defenses to adversarial examples. *arXiv preprint arXiv:1802.00420*, 2018.
- Biggio, B., Fumera, G., and Roli, F. Design of robust classifiers for adversarial environments. In *Systems, Man, and Cybernetics (SMC), 2011 IEEE International Conference on*, pp. 977–982. IEEE, 2011.
- Biggio, B., Fumera, G., and Roli, F. Security evaluation of pattern classifiers under attack. *IEEE transactions on knowledge and data engineering*, 26(4):984–996, 2014.
- Carlini, N. and Wagner, D. Towards evaluating the robustness of neural networks. In *Security and Privacy (SP), 2017 IEEE Symposium on*, pp. 39–57. IEEE, 2017a.
- Carlini, N. and Wagner, D. Adversarial examples are not easily detected: Bypassing ten detection methods. In *Proceedings of the 10th ACM Workshop on Artificial Intelligence and Security*, pp. 3–14. ACM, 2017b.
- Carlini, N. and Wagner, D. Audio adversarial examples: Targeted attacks on speech-to-text. *arXiv preprint arXiv:1801.01944*, 2018.
- Chen, P. Y., Sharma, Y., Zhang, H., Yi, J., and Hsieh, C. Ead: Elastic-net attacks to deep neural networks via adversarial examples. *arXiv preprint arXiv:1709.0414*, 2017a.
- Chen, P. Y., Zhang, H., Sharma, Y., Yi, J., and Hsieh, C. Zoo: Zeroth order optimization based black-box attacks to deep neural networks without training substitute models. In *Proceedings of the 10th ACM Workshop on Artificial Intelligence and Security*, pp. 15–26. ACM, 2017b.
- Creswell, A., Bharath, A. A., and Sengupta, B. Latentpoison-adversarial attacks on the latent space. *arXiv preprint arXiv:1711.02879*, 2017.
- Dalvi, N., Domingos, P., Sanghai, S., Verma, D., et al. Adversarial classification. In *Proceedings of the tenth ACM SIGKDD international conference on Knowledge discovery and data mining*, pp. 99–108. ACM, 2004.
- Dong, Y., Liao, F., Pang, T., Hu, X., and Zhu, J. Discovering adversarial examples with momentum. *arXiv preprint arXiv:1710.06081*, 2017.
- Efron, B. The efficiency of logistic regression compared to normal discriminant analysis. *Journal of the American Statistical Association*, 70(352):892–898, 1975.
- Feinman, R., Curtin, R. R., Shintre, S., and Gardner, A. B. Detecting adversarial samples from artifacts. *arXiv preprint arXiv:1703.00410*, 2017.
- Fisher, R. A. The use of multiple measurements in taxonomic problems. *Annals of human genetics*, 7(2):179–188, 1936.
- Gilmer, J., Metz, L., Faghri, F., Schoenholz, S. S., Raghu, M., Wattenberg, M., and Goodfellow, I. Adversarial spheres. *arXiv preprint arXiv:1801.02774*, 2018.
- Goodfellow, I. J., Shlens, J., and Szegedy, C. Explaining and harnessing adversarial examples. *arXiv preprint arXiv:1412.6572*, 2014.
- Gu, S. and Rigazio, L. Towards deep neural network architectures robust to adversarial examples. *arXiv preprint arXiv:1412.5068*, 2014.
- Huang, L., Joseph, A. D., Nelson, B., Rubinstein, B. I., and Tygar, J. Adversarial machine learning. In *Proceedings of the 4th ACM workshop on Security and artificial intelligence*, pp. 43–58. ACM, 2011.
- Kingma, D. P. and Welling, M. Auto-encoding variational bayes. *arXiv preprint arXiv:1312.6114*, 2013.
- Kos, J., Fischer, I., and Song, D. Adversarial examples for generative models. *arXiv preprint arXiv:1702.06832*, 2017.
- Kurakin, A., Goodfellow, I., and Bengio, S. Adversarial examples in the physical world. *arXiv preprint arXiv:1607.02533*, 2016.
- Kurakin, A., Goodfellow, I., Bengio, S., Dong, Y., Liao, F., Liang, M., Pang, T., Zhu, J., Hu, X., Xie, C., et al. Adversarial attacks and defences competition. *arXiv preprint arXiv:1804.00097*, 2018.
- Larsen, A. B. L., Sønderby, S. K., Larochelle, H., and Winther, O. Autoencoding beyond pixels using a learned similarity metric. In *International Conference on Machine Learning*, pp. 1558–1566, 2016.

- Li, Y. and Gal, Y. Dropout inference in bayesian neural networks with alpha-divergences. In *International Conference on Machine Learning*, pp. 2052–2061, 2017.
- Louizos, C. and Welling, M. Multiplicative normalizing flows for variational bayesian neural networks. *arXiv preprint arXiv:1703.01961*, 2017.
- Madry, A., Makelov, A., Schmidt, L., Tsipras, D., and Vladu, A. Towards deep learning models resistant to adversarial attacks. *International Conference on Learning Representations*, 2018. URL <https://openreview.net/forum?id=rJzIBfZAb>.
- Ng, A. Y. and Jordan, M. I. On discriminative vs. generative classifiers: A comparison of logistic regression and naive bayes. In *Advances in neural information processing systems*, pp. 841–848, 2002.
- Papernot, N. and McDaniel, P. Deep k-nearest neighbors: Towards confident, interpretable and robust deep learning. *arXiv preprint arXiv:1803.04765*, 2018.
- Papernot, N., McDaniel, P., and Goodfellow, I. Transferability in machine learning: from phenomena to black-box attacks using adversarial samples. *arXiv preprint arXiv:1605.07277*, 2016a.
- Papernot, N., McDaniel, P., Jha, S., Fredrikson, M., Celik, Z. B., and Swami, A. The limitations of deep learning in adversarial settings. In *Security and Privacy (EuroS&P), 2016 IEEE European Symposium on*, pp. 372–387. IEEE, 2016b.
- Papernot, N., Carlini, N., Goodfellow, I., Feinman, R., Faghri, F., Matyasko, A., Hambardzumyan, K., Juang, Y.-L., Kurakin, A., Sheatsley, R., Garg, A., and Lin, Y.-C. cleverhans v2.0.0: an adversarial machine learning library. *arXiv preprint arXiv:1610.00768*, 2017a.
- Papernot, N., McDaniel, P., Goodfellow, I., Jha, S., Celik, Z. B., and Swami, A. Practical black-box attacks against machine learning. In *Proceedings of the 2017 ACM on Asia Conference on Computer and Communications Security*, pp. 506–519. ACM, 2017b.
- Rezende, D. J., Mohamed, S., and Wierstra, D. Stochastic backpropagation and approximate inference in deep generative models. In *International Conference on Machine Learning*, pp. 1278–1286, 2014.
- Salimans, T., Karpathy, A., Chen, X., and Kingma, D. P. Pixelcnn++: Improving the pixelcnn with discretized logistic mixture likelihood and other modifications. *arXiv preprint arXiv:1701.05517*, 2017.
- Samangouei, P., Kabkab, M., and Chellappa, R. DefenseGAN: Protecting classifiers against adversarial attacks using generative models. In *International Conference on Learning Representations*, 2018. URL <https://openreview.net/forum?id=BkJ3ibb0->.
- Song, Y., Kim, T., Nowozin, S., Ermon, S., and Kushman, N. Pixeldefend: Leveraging generative models to understand and defend against adversarial examples. *International Conference on Learning Representations*, 2018. URL <https://openreview.net/forum?id=rJUYGxbCW>.
- Szegedy, C., Zaremba, W., Sutskever, I., Bruna, J., Erhan, D., Goodfellow, I., and Fergus, R. Intriguing properties of neural networks. *arXiv preprint arXiv:1312.6199*, 2013.
- Tabacof, P., Tavares, J., and Valle, E. Adversarial images for variational autoencoders. *arXiv preprint arXiv:1612.00155*, 2016.
- Tramèr, F., Kurakin, A., Papernot, N., Goodfellow, I., Boneh, D., and McDaniel, P. Ensemble adversarial training: Attacks and defenses. *arXiv preprint arXiv:1705.07204*, 2017.
- van den Oord, A., Kalchbrenner, N., and Kavukcuoglu, K. Pixel recurrent neural networks. In *International Conference on Machine Learning*, pp. 1747–1756, 2016.

## A. Model architectures

**MNIST experiments** The VAEs are constructed with convolutional encoders and deconvolutional generators. More specifically, the encoder network for  $q(\mathbf{z}|\mathbf{x}, \mathbf{y})$  is the same across all VAE-based classifiers. It starts with a 3-layer convolutional neural network with  $5 \times 5$  filters and 64 channels, with a max-pooling operation after each convolution. Then, the convolutional network is followed by a MLP with 2 hidden layers, each with 500 units, to produce the mean and variance parameters of  $q$ . The label  $\mathbf{y}$  is injected into the MLP at the first hidden layer, as a one hot encoding (i.e. for MNIST, the first hidden layer has 500+10 units). The latent dimension is  $\dim(\mathbf{z}) = 64$ .

The  $p$  models' architectures are the following:

- **GFZ**: For  $p(\mathbf{y}|\mathbf{z})$  we use a MLP with 1 hidden layer composed of 500 units. For  $p(\mathbf{x}|\mathbf{y}, \mathbf{z})$  we used a MLP with 2 hidden layers, each with 500 units, and  $4 \times 4 \times 64$  dimension output, followed by a 3-layer deconvolutional network with  $5 \times 5$  kernel size, stride 2 and [64, 64, 1] channels.
- **GFY**: We use a MLP with 1 hidden layer composed of 500 units for  $p(\mathbf{z}|\mathbf{y})$ , and the same architecture as **GFZ** for  $p(\mathbf{x}|\mathbf{y}, \mathbf{z})$ .
- **DFZ**: We use almost the same deconvolutional network architecture for  $p(\mathbf{x}|\mathbf{z})$  as **GFZ**'s  $p(\mathbf{x}|\mathbf{y}, \mathbf{z})$  network, except that the input is  $\mathbf{z}$  only. For  $p(\mathbf{y}|\mathbf{x}, \mathbf{z})$  we use almost the same architecture as  $q(\mathbf{z}|\mathbf{x}, \mathbf{y})$  except that the injected input to the MLP is  $\mathbf{z}$  and the MLP output is the set of logit values for  $\mathbf{y}$ .
- **DFX**: We use the same architecture as **G3** for  $p(\mathbf{y}|\mathbf{x}, \mathbf{z})$ . The network for  $p(\mathbf{z}|\mathbf{x})$  is almost identical except that there is no injected input to the MLP, and the network returns the mean and variance parameters for  $q(\mathbf{z}|\mathbf{x})$ .
- **DBX**: We use **GFZ**'s architecture for  $p(\mathbf{y}|\mathbf{z})$  and **DFX**'s architecture for  $p(\mathbf{z}|\mathbf{x})$ .
- **GBY**: We use **GFY**'s architecture for  $p(\mathbf{z}|\mathbf{y})$  and **DFZ**'s architecture for  $p(\mathbf{x}|\mathbf{z})$ .
- **GBZ**: We use **GFZ**'s architecture for  $p(\mathbf{y}|\mathbf{z})$  and **DFZ**'s architecture for  $p(\mathbf{x}|\mathbf{z})$ .

The BNN has almost the same architecture as the encoder network  $q$ , except that it uses 2x the hidden units/channels, and the last layer is 10 dimensions. Note that here we used dropout as it is convenient to implement, and we expect better approximate inference methods (such as stochastic gradient MCMC) to return better results for robustness and detection.

**CIFAR experiments** The model architectures are almost the same as used in MNIST experiments, except that the hidden layer dimensions for the MLP layers are increased to 1000. For the encoder  $q$ , the channels are increased to [64, 128, 256]. For the  $p$  models, the deconvolutional networks have different channel values, [128, 64, 1], and the MLP before the deconvolution outputs a  $4 \times 4 \times 256$  vector (before reshaping). The BNN has 2x the channels but still uses 1000 hidden units.

## B. Attack parameters

We use the Cleverhans package to perform attacks. We use the default hyper-parameters, if not specifically stated.

**PGD**: We perform the attack for 40 iterations with step-size 0.01.

**MIM**: We perform the attack for 40 iterations with step-size 0.01 and decay factor 1.0.

**CW- $\ell_2$** : We use learning rate 0.01 and confidence 0, and we optimise the loss for 1000 iterations.

## Are Generative Classifiers More Robust to Adversarial Attacks?

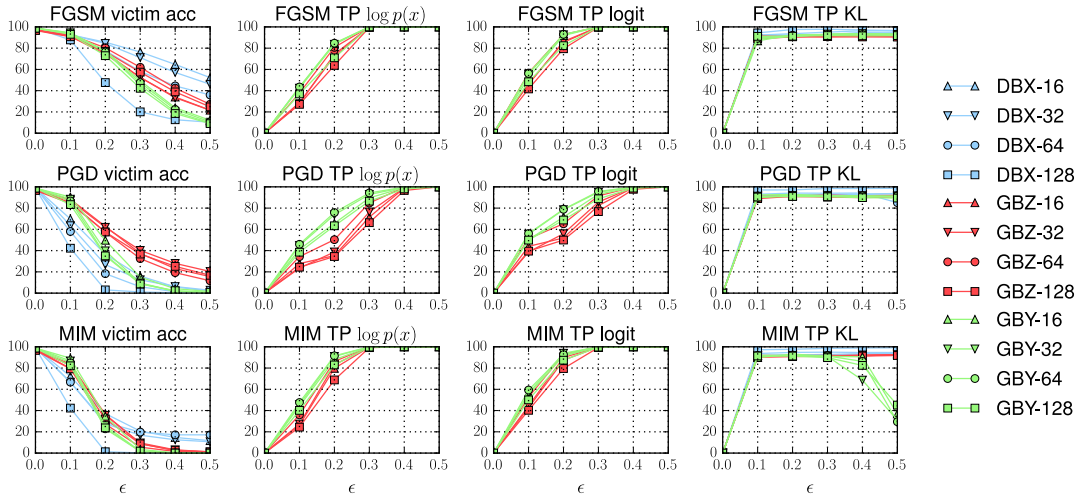


Figure C.1. Accuracy and detection rates against **white-box**  $\ell_\infty$  attacks on MNIST, with varied bottleneck layer sizes.

Table C.1. Clean test accuracy on MNIST classification (with varied bottleneck layer sizes).

	$\dim(z) = 16$	$\dim(z) = 32$	$\dim(z) = 64$	$\dim(z) = 128$
<b>DBX</b>	99.11%	99.01%	98.98%	98.91%
<b>GBZ</b>	97.11%	97.08%	97.45%	96.62%
<b>GBY</b>	98.82%	98.95%	98.72%	98.75%

Table C.2. FGSM attack results on MNIST (with varied bottleneck layer sizes).

$\epsilon$	acc. (adv)					TP marginal					TP logit					TP KL				
	0.10	0.20	0.30	0.40	0.50	0.10	0.20	0.30	0.40	0.50	0.10	0.20	0.30	0.40	0.50	0.10	0.20	0.30	0.40	0.50
DBX-16	92.6	85.6	76.4	64.7	52.3	N/A	N/A	N/A	N/A	N/A	N/A	N/A	N/A	N/A	N/A	90.3	92.4	92.3	92.7	94.2
DBX-32	92.6	84.4	71.1	57.2	46.0	N/A	N/A	N/A	N/A	N/A	N/A	N/A	N/A	N/A	N/A	92.2	92.3	92.8	94.9	95.0
DBX-64	91.6	77.8	58.1	44.5	36.0	N/A	N/A	N/A	N/A	N/A	N/A	N/A	N/A	N/A	N/A	92.3	93.6	95.1	96.4	96.7
DBX-128	87.8	47.6	20.1	12.7	10.3	N/A	N/A	N/A	N/A	N/A	N/A	N/A	N/A	N/A	N/A	94.4	97.6	97.8	97.1	96.4
GBZ-16	92.0	75.8	52.5	34.0	21.7	28.8	72.5	99.9	100.0	100.0	46.7	85.4	99.9	100.0	100.0	91.4	90.9	91.0	91.5	91.1
GBZ-32	91.1	74.4	52.4	33.4	21.6	27.7	74.3	99.7	100.0	100.0	46.1	86.3	99.9	100.0	100.0	91.1	90.5	91.9	91.7	91.5
GBZ-64	92.5	80.3	62.0	42.4	27.2	37.8	80.8	100.0	100.0	100.0	56.6	92.9	100.0	100.0	100.0	90.8	90.9	90.5	91.0	91.5
GBZ-128	90.8	76.8	57.5	38.9	24.8	27.1	63.8	99.6	100.0	100.0	41.7	79.5	99.8	100.0	100.0	88.7	90.7	90.9	90.6	90.4
GBY-16	94.2	77.7	49.4	23.9	12.1	43.2	84.4	99.9	100.0	100.0	52.3	91.9	100.0	100.0	100.0	86.8	92.6	92.9	93.6	93.3
GBY-32	94.5	76.9	45.4	20.0	9.6	42.3	83.6	100.0	100.0	100.0	55.6	92.6	100.0	100.0	100.0	88.9	90.8	93.3	93.7	92.9
GBY-64	93.6	76.4	47.5	22.3	10.7	43.5	84.7	100.0	100.0	100.0	56.2	93.0	100.0	100.0	100.0	89.3	92.1	92.8	92.8	93.1
GBY-128	93.0	72.9	42.2	18.5	9.0	37.0	70.9	100.0	100.0	100.0	48.4	82.3	99.9	100.0	100.0	91.1	91.2	91.8	91.6	91.8

## C. Further experiments

### C.1. Quantifying the effect of the bottleneck layer

We see from the main text that classifiers with bottleneck structure may be preferred for resisting adversarial examples. To quantify this bottleneck effect, we train on MNIST models **DBX**, **GBZ** and **GBY** with  $z$  dimensions in  $\{16, 32, 64, 128\}$  (the main text experiments use  $\dim(z) = 64$ ). The clean accuracy on test data is shown in Table C.1, and we see all the models in test perform reasonably well.

We repeat the same white-box  $\ell_\infty$  attack experiments as done in the main text, where results are presented in Figure C.1 and Tables C.2, C.3 and C.4. It is clear that for discriminative classifiers **DBX** the model becomes less robust as the bottleneck dimension  $\dim(z)$  increases. Interestingly **DBX** classifiers seem to be very robust against FGSM attacks, which agrees with the results in [Alemi et al. \(2017\)](#). For the generative ones, we also observe similar trends (although much less significant) of decreased robustness for **GBY** classifiers, and for **GBZ** the trend is unclear, presumably due to local optimum issues in optimisation. In sum, **GBZ** classifiers are generally more robust compared to **GBY** classifiers. More importantly, when the accuracy of generative classifiers on adversarial images decreases to zero, the detection rates with marginal/logit detection increases to 100%. This clearly shows that the three attacks tested here cannot fool the generative classifiers without being detected.

Are Generative Classifiers More Robust to Adversarial Attacks?

Table C.3. PGD attack results on MNIST (with varied bottleneck layer sizes).

$\epsilon$	acc. (adv)					TP marginal					TP logit					TP KL				
	0.10	0.20	0.30	0.40	0.50	0.10	0.20	0.30	0.40	0.50	0.10	0.20	0.30	0.40	0.50	0.10	0.20	0.30	0.40	0.50
DBX-16	69.8	36.6	16.0	5.9	1.8	N/A	N/A	N/A	N/A	N/A	N/A	N/A	N/A	N/A	N/A	91.2	91.9	92.8	93.3	93.7
DBX-32	63.5	26.8	12.5	6.2	2.7	N/A	N/A	N/A	N/A	N/A	N/A	N/A	N/A	N/A	N/A	91.5	92.1	92.7	92.9	93.5
DBX-64	58.0	18.3	6.0	1.3	0.2	N/A	N/A	N/A	N/A	N/A	N/A	N/A	N/A	N/A	N/A	93.0	94.1	94.0	94.2	85.1
DBX-128	42.3	3.0	1.1	0.3	0.2	N/A	N/A	N/A	N/A	N/A	N/A	N/A	N/A	N/A	N/A	97.1	97.1	98.4	98.4	98.6
GBZ-16	88.3	62.8	37.4	23.1	15.5	27.8	35.3	71.5	98.9	100.0	44.0	51.9	82.4	99.3	100.0	90.5	91.6	91.9	91.7	92.0
GBZ-32	87.1	61.9	40.2	28.0	20.4	23.5	38.7	76.4	99.1	100.0	38.7	55.9	85.7	99.6	100.0	91.3	90.7	91.3	91.6	91.4
GBZ-64	85.1	57.4	32.5	19.3	11.6	34.3	50.3	84.8	99.7	100.0	51.3	65.2	91.5	99.8	100.0	90.2	91.4	92.2	91.4	91.6
GBZ-128	84.4	57.5	36.8	25.2	16.8	24.4	34.5	66.3	96.6	100.0	39.5	50.0	76.7	97.7	100.0	88.9	91.1	90.3	89.9	90.6
GBY-16	90.4	49.7	15.0	4.2	1.6	41.2	65.6	89.6	99.4	100.0	50.3	71.6	93.1	99.4	100.0	92.4	92.8	91.7	91.1	91.1
GBY-32	88.4	39.8	9.5	1.8	0.6	44.8	73.7	92.8	99.5	100.0	55.4	78.5	94.9	99.8	100.0	90.7	91.8	91.7	91.4	90.7
GBY-64	86.7	35.9	9.0	1.7	0.4	45.9	75.8	94.3	99.8	100.0	56.0	78.9	95.7	99.9	100.0	89.8	92.1	91.3	91.4	91.3
GBY-128	83.3	35.1	8.7	2.3	0.8	38.5	63.4	86.5	98.1	99.9	49.9	68.8	88.8	98.8	99.9	90.4	90.9	90.7	89.9	89.4

Table C.4. MIM attack results on MNIST (with varied bottleneck layer sizes).

$\epsilon$	acc. (adv)					TP marginal					TP logit					TP KL				
	0.10	0.20	0.30	0.40	0.50	0.10	0.20	0.30	0.40	0.50	0.10	0.20	0.30	0.40	0.50	0.10	0.20	0.30	0.40	0.50
DBX-16	72.2	37.1	20.7	14.7	11.7	N/A	N/A	N/A	N/A	N/A	N/A	N/A	N/A	N/A	N/A	91.8	92.3	92.8	93.4	93.9
DBX-32	66.7	27.6	16.8	12.5	10.6	N/A	N/A	N/A	N/A	N/A	N/A	N/A	N/A	N/A	N/A	91.8	92.5	92.4	93.2	93.5
DBX-64	66.7	28.7	19.7	17.2	17.2	N/A	N/A	N/A	N/A	N/A	N/A	N/A	N/A	N/A	N/A	93.7	94.7	94.9	94.6	94.6
DBX-128	42.3	1.3	0.2	0.1	0.0	N/A	N/A	N/A	N/A	N/A	N/A	N/A	N/A	N/A	N/A	97.2	97.6	98.6	98.9	99.1
GBZ-16	83.8	36.4	8.9	2.3	0.9	26.3	79.7	99.7	100.0	100.0	42.7	87.4	99.8	100.0	100.0	91.9	91.6	91.5	91.5	92.6
GBZ-32	82.7	35.5	9.5	3.0	1.1	27.3	83.1	99.7	100.0	100.0	44.2	89.9	99.8	100.0	100.0	91.2	91.6	91.2	92.3	92.6
GBZ-64	79.6	27.4	5.6	1.5	0.5	35.9	86.2	100.0	100.0	100.0	52.6	93.0	99.9	100.0	100.0	91.2	91.7	91.9	91.8	92.4
GBZ-128	79.2	32.1	8.7	2.6	1.2	24.4	68.8	99.2	100.0	100.0	40.2	79.5	99.3	100.0	100.0	90.1	90.7	91.2	91.3	91.8
GBY-16	89.2	34.6	3.5	0.2	0.0	44.1	87.9	99.8	100.0	100.0	55.0	91.4	99.7	100.0	100.0	89.8	93.2	91.0	90.6	36.9
GBY-32	86.7	25.8	1.6	0.1	0.0	45.6	90.9	99.9	100.0	100.0	56.3	93.9	99.9	100.0	100.0	91.3	91.7	90.9	68.7	30.9
GBY-64	84.9	22.9	1.5	0.1	0.0	47.5	91.5	99.9	100.0	100.0	59.3	92.6	99.9	100.0	100.0	91.9	92.0	91.3	86.3	29.5
GBY-128	82.1	23.7	1.9	0.0	0.0	40.2	82.9	99.7	100.0	100.0	50.1	87.4	99.7	100.0	100.0	91.3	91.3	89.8	82.5	45.1

## Are Generative Classifiers More Robust to Adversarial Attacks?

*Table D.1. FGSM white-box attack results on MNIST.*

$\epsilon$	acc. (adv)					TP marginal					TP logit					TP KL				
	0.10	0.20	0.30	0.40	0.50	0.10	0.20	0.30	0.40	0.50	0.10	0.20	0.30	0.40	0.50	0.10	0.20	0.30	0.40	0.50
BNN	92.4	67.8	40.5	26.2	20.4	N/A	N/A	N/A	N/A	N/A	N/A	N/A	N/A	N/A	N/A	93.0	94.2	95.4	95.5	96.5
GFZ	94.2	74.5	38.9	12.9	5.7	43.9	80.1	99.9	100.0	100.0	54.7	88.9	100.0	100.0	100.0	89.4	91.9	92.5	92.4	92.4
GBZ	92.5	80.3	62.0	42.4	27.2	37.8	80.8	100.0	100.0	100.0	56.6	92.9	100.0	100.0	100.0	90.8	90.9	90.5	91.0	91.5
GFY	94.3	74.8	46.5	21.7	10.5	51.9	92.0	100.0	100.0	100.0	64.1	97.7	100.0	100.0	100.0	90.6	93.0	93.7	94.3	94.9
GBY	93.6	76.4	47.5	22.3	10.7	43.5	84.7	100.0	100.0	100.0	56.2	93.0	100.0	100.0	100.0	89.3	92.1	92.8	92.8	93.1
DFX	70.1	14.8	1.0	0.4	0.6	N/A	N/A	N/A	N/A	N/A	N/A	N/A	N/A	N/A	N/A	93.6	93.9	93.9	93.5	94.3
DBX	91.6	77.8	58.1	44.5	36.0	N/A	N/A	N/A	N/A	N/A	N/A	N/A	N/A	N/A	N/A	92.3	93.6	95.1	96.4	96.7
DFZ	75.2	19.0	2.4	1.1	1.0	12.6	50.0	100.0	100.0	100.0	24.5	65.9	100.0	100.0	100.0	92.8	95.2	94.5	94.7	94.9

*Table D.2. PGD white-box attack results on MNIST.*

$\epsilon$	acc. (adv)					TP marginal					TP logit					TP KL				
	0.10	0.20	0.30	0.40	0.50	0.10	0.20	0.30	0.40	0.50	0.10	0.20	0.30	0.40	0.50	0.10	0.20	0.30	0.40	0.50
BNN	83.2	12.0	0.5	0.0	0.0	N/A	N/A	N/A	N/A	N/A	N/A	N/A	N/A	N/A	N/A	92.1	92.1	88.7	20.4	0.2
GFZ	86.7	37.7	7.7	1.2	0.3	42.8	72.5	91.4	99.4	100.0	54.8	77.4	94.8	99.6	100.0	90.5	92.2	90.8	90.7	89.6
GBZ	85.1	57.4	32.5	19.3	11.6	34.3	50.3	84.8	99.7	100.0	51.3	65.2	91.5	99.8	100.0	90.2	91.4	92.2	91.4	91.6
GFY	79.7	27.4	5.6	1.2	0.3	58.1	88.0	98.0	100.0	100.0	67.5	91.8	99.1	100.0	100.0	92.7	92.1	90.4	90.6	85.5
GBY	86.7	35.9	9.0	1.7	0.4	45.9	75.8	94.3	99.8	100.0	56.0	78.9	95.7	99.9	100.0	89.8	92.1	91.3	91.4	91.3
DFX	47.6	0.7	0.0	0.0	0.0	N/A	N/A	N/A	N/A	N/A	N/A	N/A	N/A	N/A	N/A	92.7	89.8	13.3	31.1	42.3
DBX	58.0	18.3	6.0	1.3	0.2	N/A	N/A	N/A	N/A	N/A	N/A	N/A	N/A	N/A	N/A	93.0	94.1	94.0	94.2	85.1
DFZ	49.6	1.0	0.0	0.0	0.0	11.6	44.2	94.0	100.0	100.0	24.0	57.2	94.7	99.9	100.0	94.0	89.8	12.1	23.1	27.5

*Table D.3. MIM white-box attack results on MNIST.*

$\epsilon$	acc. (adv)					TP marginal					TP logit					TP KL				
	0.10	0.20	0.30	0.40	0.50	0.10	0.20	0.30	0.40	0.50	0.10	0.20	0.30	0.40	0.50	0.10	0.20	0.30	0.40	0.50
BNN	82.0	7.2	0.1	0.0	0.0	N/A	N/A	N/A	N/A	N/A	N/A	N/A	N/A	N/A	N/A	92.2	91.1	72.0	64.5	7.1
GFZ	87.0	40.4	9.0	1.2	1.2	43.7	83.9	98.4	99.3	99.3	55.4	89.3	98.6	99.1	99.1	91.6	92.2	92.0	90.8	90.8
GBZ	79.6	27.4	5.6	1.5	0.5	35.9	86.2	100.0	100.0	100.0	52.6	93.0	99.9	100.0	100.0	91.2	91.7	91.9	91.8	92.4
GFY	80.8	30.1	6.8	1.4	1.4	56.3	93.3	99.8	100.0	100.0	67.7	96.8	99.8	100.0	100.0	90.7	92.4	92.3	91.6	91.6
GBY	84.9	22.9	1.5	0.1	0.0	47.5	91.5	99.9	100.0	100.0	59.3	92.6	99.9	100.0	100.0	91.9	92.0	91.3	86.3	29.5
DFX	48.4	0.8	0.0	0.0	0.0	N/A	N/A	N/A	N/A	N/A	N/A	N/A	N/A	N/A	N/A	93.2	89.6	9.1	17.6	17.6
DBX	66.7	28.7	19.7	17.2	17.2	N/A	N/A	N/A	N/A	N/A	N/A	N/A	N/A	N/A	N/A	93.7	94.7	94.9	94.6	94.6
DFZ	50.5	1.2	0.0	0.0	0.0	11.9	50.5	99.3	100.0	100.0	24.9	63.1	99.1	100.0	100.0	94.3	89.7	11.7	17.3	17.3

*Table D.4. FGSM white-box attack results on CIFAR plane-vs-frog binary classification.*

$\epsilon$	acc. (adv)					TP marginal					TP logit					TP KL				
	0.01	0.02	0.05	0.10	0.20	0.01	0.02	0.05	0.10	0.20	0.01	0.02	0.05	0.10	0.20	0.01	0.02	0.05	0.10	0.20
BNN	98.2	93.2	58.5	14.5	6.3	N/A	N/A	N/A	N/A	N/A	N/A	N/A	N/A	N/A	N/A	58.6	55.1	65.5	54.0	58.5
GFZ	97.1	94.7	81.8	56.4	31.4	11.4	7.6	6.6	17.3	99.2	11.4	10.4	6.8	17.9	99.3	56.8	42.3	36.3	39.8	51.6
GBZ	95.1	93.5	87.1	74.9	62.0	26.0	19.6	15.5	37.8	99.6	27.4	21.1	17.7	42.0	99.6	37.7	40.7	43.9	46.8	42.1
GFY	96.5	94.2	80.7	56.7	32.0	9.6	8.0	6.6	18.8	98.8	17.6	13.1	7.9	21.9	99.1	46.6	40.1	39.8	40.8	47.6
GBY	96.1	92.9	82.0	60.5	36.3	15.5	15.1	8.5	27.2	99.1	20.2	17.4	10.2	28.7	99.2	46.8	41.7	40.5	38.9	50.5
DFX	83.8	42.2	0.7	0.0	0.0	N/A	N/A	N/A	N/A	N/A	N/A	N/A	N/A	N/A	N/A	63.3	66.9	48.6	97.7	100.0
DBX	90.9	78.6	50.7	31.7	18.3	N/A	N/A	N/A	N/A	N/A	N/A	N/A	N/A	N/A	N/A	55.3	61.2	57.2	59.7	57.1
DFZ	83.9	52.1	2.9	0.0	0.0	6.2	3.5	2.1	3.9	61.1	6.9	4.3	2.2	3.7	60.2	58.0	62.1	54.9	67.7	99.7

### D. Main text results in tables

#### D.1. Tables for the white-box attacks

See Tables D.1 to D.7.

#### D.2. Tables for the grey-box attacks

See Tables D.8 to D.13.

#### D.3. Tables for the black-box attacks

See Tables D.14 to D.19.

**Are Generative Classifiers More Robust to Adversarial Attacks?**

*Table D.5. PGD white-box attack results on CIFAR plane-vs-frog binary classification.*

$\epsilon$	acc. (adv)					TP marginal					TP logit					TP KL				
	0.01	0.02	0.05	0.10	0.20	0.01	0.02	0.05	0.10	0.20	0.01	0.02	0.05	0.10	0.20	0.01	0.02	0.05	0.10	0.20
BNN	97.9	86.7	19.7	1.0	0.0	N/A	N/A	N/A	N/A	N/A	N/A	N/A	N/A	N/A	41.7	59.4	55.7	68.4	98.9	
GFZ	98.0	93.9	67.7	21.7	3.5	3.3	6.6	4.7	7.9	32.9	5.0	9.5	5.8	8.2	33.8	37.5	46.6	34.8	41.0	56.5
GBZ	94.6	93.7	83.9	67.4	52.8	18.5	17.9	12.8	14.7	42.4	21.2	19.5	16.2	17.3	44.2	33.7	39.0	41.0	31.3	30.3
GFY	98.4	95.0	67.9	25.8	4.1	4.2	5.3	6.2	7.6	35.6	3.1	8.2	7.8	8.1	34.3	31.2	38.6	34.8	39.2	54.2
GBY	96.4	92.9	67.3	25.7	6.9	7.4	8.4	8.1	11.3	41.0	13.1	11.5	8.9	11.9	39.5	38.4	39.0	35.8	39.6	52.2
DFX	82.7	35.7	0.3	0.0	0.0	N/A	N/A	N/A	N/A	N/A	N/A	N/A	N/A	N/A	64.1	64.8	69.6	100.0	100.0	
DBX	83.3	34.6	4.2	0.7	0.0	N/A	N/A	N/A	N/A	N/A	N/A	N/A	N/A	N/A	61.1	59.7	65.0	81.6	93.0	
DFZ	82.4	36.9	0.4	0.0	0.0	4.9	3.6	5.0	12.6	91.3	6.5	4.0	5.7	12.2	91.0	58.2	59.7	52.8	99.8	100.0

*Table D.6. MIM white-box attack results on CIFAR plane-vs-frog binary classification.*

$\epsilon$	acc. (adv)					TP marginal					TP logit					TP KL				
	0.01	0.02	0.05	0.10	0.20	0.01	0.02	0.05	0.10	0.20	0.01	0.02	0.05	0.10	0.20	0.01	0.02	0.05	0.10	0.20
BNN	96.9	84.6	18.7	0.9	0.0	N/A	N/A	N/A	N/A	N/A	N/A	N/A	N/A	N/A	35.9	54.7	56.3	62.4	78.8	
GFZ	96.9	91.5	58.1	15.2	1.9	6.5	6.2	5.4	10.9	86.1	10.0	8.3	7.0	11.7	84.7	34.0	39.5	35.6	47.0	77.3
GBZ	92.5	89.4	71.5	40.4	17.9	15.0	14.5	10.5	23.5	95.6	16.4	14.8	13.0	24.7	95.7	39.6	38.9	33.4	37.4	54.5
GFY	97.6	92.3	59.5	16.5	2.3	5.6	6.9	6.3	13.9	87.6	5.7	6.9	7.1	14.1	87.8	26.2	38.9	34.7	40.7	74.9
GBY	95.1	88.8	56.5	14.6	1.3	12.3	9.5	8.6	18.3	96.6	13.0	10.2	10.0	18.2	96.4	43.6	40.2	34.7	48.2	86.6
DFX	82.5	35.2	0.3	0.0	0.0	N/A	N/A	N/A	N/A	N/A	N/A	N/A	N/A	N/A	65.5	67.3	69.7	100.0	100.0	
DBX	82.5	38.8	6.1	1.2	0.1	N/A	N/A	N/A	N/A	N/A	N/A	N/A	N/A	N/A	56.7	60.5	62.8	80.4	89.2	
DFZ	81.5	36.1	0.4	0.0	0.0	5.0	3.6	5.0	13.6	96.9	6.2	4.0	5.7	14.0	96.9	63.4	59.1	54.1	99.8	100.0

*Table D.7. CW white-box attack results on CIFAR plane-vs-frog binary classification.*

$c$	acc. (adv)					TP marginal					TP logit					TP KL				
	0.1	1	10	100	1000	0.1	1	10	100	1000	0.1	1	10	100	1000	0.1	1	10	100	1000
BNN	93.7	66.2	37.3	32.3	47.6	N/A	N/A	N/A	N/A	N/A	N/A	N/A	N/A	N/A	60.9	80.3	82.2	72.0	80.0	
GFZ	99.5	95.6	76.5	77.9	78.3	0.0	6.1	2.3	2.7	3.1	0.0	4.6	2.7	2.9	3.5	45.8	35.2	27.0	26.6	25.8
GBZ	96.0	93.6	88.9	88.7	89.0	16.7	11.5	7.8	7.7	7.9	18.9	12.8	8.8	8.6	8.8	43.1	51.6	32.5	29.7	26.0
GFY	99.8	95.9	78.8	80.0	80.5	0.0	4.9	4.1	4.3	4.4	0.0	6.6	5.4	5.6	5.7	50.0	37.3	28.8	24.0	26.7
GBY	97.5	93.1	76.7	77.3	78.0	15.8	12.6	5.4	6.2	6.7	18.9	15.8	6.3	7.3	7.9	45.5	35.4	32.1	30.4	29.0
DFX	82.6	44.2	34.3	6.1	0.6	N/A	N/A	N/A	N/A	N/A	N/A	N/A	N/A	N/A	N/A	100.0	100.0	100.0	82.4	95.2
DBX	96.5	72.2	26.3	6.3	16.2	N/A	N/A	N/A	N/A	N/A	N/A	N/A	N/A	N/A	N/A	57.2	83.0	88.8	64.0	69.8
DFZ	94.5	72.3	29.9	6.3	17.9	6.1	6.0	4.3	4.0	3.9	11.4	7.1	5.2	4.4	4.4	87.3	97.0	96.1	83.2	81.0

*Table D.8. Grey-box PGD attack results on MNIST.*

$\epsilon$	substitute acc					victim acc					TP logit				
	0.10	0.20	0.30	0.40	0.50	0.10	0.20	0.30	0.40	0.50	0.10	0.20	0.30	0.40	0.50
GFZ	86.8	14.5	0.0	0.0	0.0	96.2	83.5	52.0	27.1	17.2	47.1	74.0	99.8	100.0	100.0
GBZ	81.2	9.1	0.0	0.0	0.0	93.8	80.4	56.9	34.4	25.5	44.4	72.9	99.6	100.0	100.0
GFY	84.9	6.5	0.0	0.0	0.0	96.7	82.3	54.9	33.4	24.2	54.4	89.0	100.0	100.0	100.0
GBY	86.7	15.0	0.0	0.0	0.0	95.9	81.3	50.4	27.2	18.4	47.1	78.7	99.9	100.0	100.0
DFX	74.2	5.2	0.5	0.0	0.0	91.7	57.7	19.6	4.3	1.4	N/A	N/A	N/A	N/A	N/A
DBX	80.6	5.1	0.0	0.0	0.0	93.2	59.2	22.5	10.9	8.2	N/A	N/A	N/A	N/A	N/A
DFZ	69.5	3.5	0.2	0.0	0.0	92.0	56.9	21.5	6.8	2.9	30.5	53.8	91.7	100.0	100.0

*Table D.9. Grey-box MIM attack results on MNIST.*

$\epsilon$	substitute acc					victim acc					TP logit				
	0.10	0.20	0.30	0.40	0.50	0.10	0.20	0.30	0.40	0.50	0.10	0.20	0.30	0.40	0.50
GFZ	87.6	24.6	1.1	0.3	0.3	96.2	82.1	44.1	16.8	16.8	46.5	79.5	99.9	100.0	100.0
GBZ	81.8	9.1	0.0	0.0	0.0	93.6	79.0	45.6	17.4	5.1	42.6	81.3	100.0	100.0	100.0
GFY	85.9	14.2	0.8	0.2	0.2	96.6	80.6	49.5	23.4	23.4	56.9	95.1	100.0	100.0	100.0
GBY	87.0	15.9	0.0	0.0	0.0	96.0	79.7	41.6	13.1	3.9	48.1	86.7	100.0	100.0	100.0
DFX	76.5	12.3	3.6	2.1	2.1	91.5	56.1	22.2	9.9	9.9	N/A	N/A	N/A	N/A	N/A
DBX	85.1	19.9	0.6	0.1	0.1	93.4	57.0	14.1	6.3	6.3	N/A	N/A	N/A	N/A	N/A
DFZ	72.3	7.4	1.4	0.8	0.8	91.7	56.4	20.9	8.4	8.4	32.3	63.3	98.9	100.0	100.0

**Are Generative Classifiers More Robust to Adversarial Attacks?**

*Table D.10. Grey-box CW attack results on MNIST.*

$c$	substitute acc					victim acc					TP logit				
	0.10	1.00	10.00	100.00	1000.00	0.10	1.00	10.00	100.00	1000.00	0.10	1.00	10.00	100.00	1000.00
GFZ	98.4	4.6	0.0	0.0	0.0	98.9	96.8	96.0	93.6	90.3	50.9	41.3	40.7	36.2	39.1
GBZ	98.4	63.2	0.0	0.0	0.0	97.5	95.4	93.0	89.0	84.4	47.9	39.9	31.7	30.3	36.9
GFY	98.1	0.9	0.0	0.0	0.0	99.0	97.6	97.0	95.9	94.2	54.0	42.6	43.1	42.3	48.2
GBY	98.3	5.3	0.0	0.0	0.0	98.7	97.0	96.2	93.6	90.8	45.8	38.4	35.2	37.4	42.9
DFX	85.1	0.0	0.0	0.0	0.0	97.6	93.3	91.2	90.4	89.8	N/A	N/A	N/A	N/A	N/A
DBX	97.3	46.0	0.4	0.0	0.0	98.7	93.9	88.4	85.5	76.3	N/A	N/A	N/A	N/A	N/A
DFZ	80.5	0.0	0.0	0.0	0.0	97.4	94.4	92.2	91.7	91.1	27.0	22.5	22.1	32.2	38.8

*Table D.11. Grey-box PGD attack results on CIFAR plane-vs-frog binary classification.*

$\epsilon$	substitute acc					victim acc					TP logit				
	0.01	0.02	0.05	0.10	0.20	0.01	0.02	0.05	0.10	0.20	0.01	0.02	0.05	0.10	0.20
GFZ	96.7	88.1	41.7	4.5	0.1	97.9	95.5	84.1	48.8	9.3	3.8	5.6	4.0	7.4	51.4
GBZ	92.9	83.1	37.8	5.5	0.0	94.6	93.5	90.3	82.9	65.6	17.9	17.6	15.2	20.7	80.6
GFY	96.9	88.1	33.7	3.3	0.1	97.2	95.4	85.3	54.9	13.3	7.3	5.5	6.5	8.3	61.8
GBY	95.2	85.6	32.4	2.8	0.1	96.4	94.8	86.4	59.1	17.5	16.9	13.9	8.6	11.9	74.3
DFX	95.7	80.8	10.1	0.2	0.0	99.1	96.7	79.4	28.3	0.9	N/A	N/A	N/A	N/A	N/A
DBX	95.7	80.5	30.5	1.7	0.0	99.5	98.2	91.1	65.1	21.8	N/A	N/A	N/A	N/A	N/A
DFZ	96.5	81.9	10.5	0.3	0.0	99.1	97.1	77.6	25.5	1.3	0.0	5.5	6.7	9.3	60.0

*Table D.12. Grey-box MIM attack results on CIFAR plane-vs-frog binary classification.*

$\epsilon$	substitute acc					victim acc					TP logit				
	0.01	0.02	0.05	0.10	0.20	0.01	0.02	0.05	0.10	0.20	0.01	0.02	0.05	0.10	0.20
GFZ	96.3	87.9	42.1	4.7	0.1	97.9	95.5	83.3	46.5	5.8	3.8	5.5	4.6	8.4	76.3
GBZ	92.9	82.5	36.9	4.9	0.0	94.5	93.6	90.2	80.7	51.1	17.1	16.6	16.0	21.8	98.0
GFY	96.8	87.9	34.1	3.5	0.1	97.1	95.3	84.4	49.9	7.4	7.2	5.4	6.6	10.4	81.2
GBY	95.1	85.5	32.0	2.6	0.1	96.4	94.8	85.9	54.4	10.7	16.9	13.9	8.4	13.7	97.6
DFX	95.5	80.5	10.5	0.2	0.0	99.1	96.5	77.3	24.0	0.2	N/A	N/A	N/A	N/A	N/A
DBX	95.6	81.1	34.5	2.2	0.0	99.5	98.3	89.3	58.9	9.9	N/A	N/A	N/A	N/A	N/A
DFZ	96.3	81.5	10.7	0.5	0.0	99.1	96.5	74.9	21.7	0.3	0.0	7.3	6.4	10.3	80.8

*Table D.13. Grey-box CW attack results on CIFAR plane-vs-frog binary classification.*

$c$	substitute acc					victim acc					TP logit				
	0.10	1.00	10.00	100.00	1000.00	0.10	1.00	10.00	100.00	1000.00	0.10	1.00	10.00	100.00	1000.00
GFZ	98.7	61.9	0.0	0.0	0.0	98.9	95.9	94.9	94.5	93.3	10.0	2.1	4.5	4.1	4.1
GBZ	96.3	69.8	3.3	0.0	0.0	95.3	94.9	93.6	93.5	93.5	18.2	16.9	17.9	17.3	17.3
GFY	98.4	54.4	0.0	0.0	0.0	98.4	95.9	95.0	94.9	94.2	13.0	5.5	4.1	5.0	4.4
GBY	97.6	52.9	2.2	0.0	0.0	97.9	95.1	94.1	93.8	93.3	20.9	13.0	11.1	13.1	16.2
DFX	64.4	0.0	0.0	0.0	0.0	98.5	97.2	97.1	96.7	95.5	N/A	N/A	N/A	N/A	N/A
DBX	91.3	56.2	0.3	0.0	0.0	99.7	99.0	99.0	98.9	98.1	N/A	N/A	N/A	N/A	N/A
DFZ	80.3	0.0	0.0	0.0	0.0	98.9	97.7	97.5	97.5	95.9	0.0	24.5	20.6	15.4	13.2

*Table D.14. Black-box PGD attack results on MNIST.*

$\epsilon$	substitute acc					victim acc					TP logit				
	0.10	0.20	0.30	0.40	0.50	0.10	0.20	0.30	0.40	0.50	0.10	0.20	0.30	0.40	0.50
GFZ	44.2	0.7	0.0	0.0	0.0	97.0	88.8	62.3	33.7	21.8	43.1	59.9	92.7	99.8	100.0
GBZ	7.4	0.0	0.0	0.0	0.0	95.2	87.8	71.5	53.6	42.1	43.0	68.1	98.0	100.0	100.0
GFY	49.4	0.8	0.0	0.0	0.0	97.2	86.4	57.6	32.1	21.5	49.6	71.5	97.1	99.7	100.0
GBY	21.7	0.0	0.0	0.0	0.0	96.9	89.1	70.3	49.5	38.1	46.7	69.1	98.4	100.0	100.0
DFX	49.2	1.3	0.0	0.0	0.0	91.4	52.1	13.9	2.2	0.7	N/A	N/A	N/A	N/A	N/A
DBX	43.1	0.7	0.0	0.0	0.0	95.0	67.0	26.2	9.7	6.5	N/A	N/A	N/A	N/A	N/A
DFZ	53.8	1.7	0.0	0.0	0.0	92.7	55.8	15.3	3.6	1.4	29.1	52.5	93.8	99.9	100.0



**Are Generative Classifiers More Robust to Adversarial Attacks?**

*Table D.15. Black-box MIM attack results on MNIST.*

$\epsilon$	substitute acc					victim acc					TP logit				
	0.10	0.20	0.30	0.40	0.50	0.10	0.20	0.30	0.40	0.50	0.10	0.20	0.30	0.40	0.50
GFZ	45.5	2.8	0.0	0.0	0.0	97.0	86.7	50.3	17.0	17.0	44.6	67.0	97.7	99.6	99.6
GBZ	8.4	0.0	0.0	0.0	0.0	95.2	86.7	64.2	36.4	17.0	45.5	73.0	98.9	100.0	100.0
GFY	53.1	2.5	0.3	0.1	0.1	97.1	83.8	49.0	20.5	20.5	51.9	80.5	98.9	99.9	99.9
GBY	24.5	0.0	0.0	0.0	0.0	97.0	88.5	63.1	31.8	13.1	47.3	77.0	99.8	100.0	100.0
DFX	51.3	2.3	0.1	0.0	0.0	91.4	51.7	13.3	1.9	1.9	N/A	N/A	N/A	N/A	N/A
DBX	47.8	1.6	0.1	0.0	0.0	94.8	67.0	23.2	7.6	7.6	N/A	N/A	N/A	N/A	N/A
DFZ	56.1	2.9	0.1	0.0	0.0	92.8	56.0	13.2	2.7	2.7	30.6	59.4	97.4	100.0	100.0

*Table D.16. Black-box CW attack results on MNIST.*

$c$	substitute acc					victim acc					TP logit				
	0.10	1.00	10.00	100.00	1000.00	0.10	1.00	10.00	100.00	1000.00	0.10	1.00	10.00	100.00	1000.00
GFZ	65.2	0.3	0.0	0.0	0.0	98.9	98.8	97.4	94.4	92.3	49.9	50.8	38.6	41.2	49.8
GBZ	76.6	0.4	0.0	0.0	0.0	97.3	97.0	96.1	93.2	91.0	46.5	43.6	39.0	38.2	46.0
GFY	88.4	3.8	0.0	0.0	0.0	99.1	98.9	98.0	95.3	92.3	54.0	52.8	48.4	48.9	57.5
GBY	76.0	1.3	0.0	0.0	0.0	98.6	98.5	97.3	94.9	93.2	48.5	48.4	40.1	40.2	44.5
DFX	82.4	0.0	0.0	0.0	0.0	98.8	96.8	92.4	86.2	84.9	N/A	N/A	N/A	N/A	N/A
DBX	82.5	0.6	0.0	0.0	0.0	98.9	98.4	95.5	85.2	83.1	N/A	N/A	N/A	N/A	N/A
DFZ	86.5	0.2	0.0	0.0	0.0	98.9	94.6	89.7	81.7	79.4	33.8	19.9	18.2	23.5	34.0

*Table D.17. Black-box PGD attack results on CIFAR plane-vs-frog binary classification.*

$\epsilon$	substitute acc					victim acc					TP logit				
	0.01	0.02	0.05	0.10	0.20	0.01	0.02	0.05	0.10	0.20	0.01	0.02	0.05	0.10	0.20
GFZ	95.5	89.9	45.5	6.8	0.1	98.1	96.5	89.3	69.3	30.5	4.2	3.9	6.0	10.4	72.3
GBZ	92.0	84.1	33.8	3.5	0.0	94.7	93.9	90.4	83.3	65.4	18.8	16.7	17.4	18.4	75.5
GFY	95.3	89.1	38.7	2.5	0.0	97.8	96.6	90.5	73.3	36.7	9.7	6.1	7.5	11.2	71.4
GBY	91.8	80.5	29.7	6.1	0.2	96.8	95.6	89.9	69.9	31.1	17.1	12.9	8.5	10.7	77.8
DFX	89.1	74.5	19.1	0.9	0.0	99.6	98.6	92.5	65.0	9.9	N/A	N/A	N/A	N/A	N/A
DBX	85.5	76.4	42.5	4.5	0.0	99.6	98.9	95.1	77.3	25.1	N/A	N/A	N/A	N/A	N/A
DFZ	85.5	73.5	21.1	1.5	0.0	99.6	98.9	93.8	70.2	14.8	0.0	0.0	8.3	16.0	85.4

*Table D.18. Black-box MIM attack results on CIFAR plane-vs-frog binary classification.*

$\epsilon$	substitute acc					victim acc					TP logit				
	0.01	0.02	0.05	0.10	0.20	0.01	0.02	0.05	0.10	0.20	0.01	0.02	0.05	0.10	0.20
GFZ	95.5	89.7	46.4	7.7	0.2	98.1	96.5	89.2	66.9	19.9	4.2	3.9	5.8	11.7	84.2
GBZ	91.8	84.0	33.1	3.4	0.0	94.7	93.7	90.4	82.2	60.3	18.8	16.2	17.0	21.5	97.6
GFY	95.3	88.9	40.5	3.1	0.0	97.7	96.7	90.2	71.7	33.5	8.7	6.4	7.4	11.5	87.7
GBY	91.7	80.2	29.5	5.9	0.1	96.9	95.5	89.4	68.5	24.3	17.4	12.8	8.0	11.9	95.9
DFX	89.0	74.5	19.4	0.9	0.0	99.5	98.7	91.9	62.9	10.8	N/A	N/A	N/A	N/A	N/A
DBX	85.5	76.3	42.7	4.5	0.0	99.6	98.8	95.0	76.8	26.5	N/A	N/A	N/A	N/A	N/A
DFZ	85.3	73.4	21.4	1.6	0.0	99.6	98.9	93.3	67.4	15.1	0.0	0.0	8.6	15.6	92.0

*Table D.19. Black-box CW attack results on CIFAR plane-vs-frog binary classification.*

$c$	substitute acc					victim acc					TP logit				
	0.10	1.00	10.00	100.00	1000.00	0.10	1.00	10.00	100.00	1000.00	0.10	1.00	10.00	100.00	1000.00
GFZ	96.3	41.5	0.5	0.0	0.0	98.8	95.8	94.4	94.2	93.5	8.3	3.6	6.6	6.5	7.9
GBZ	94.9	73.3	1.4	0.0	0.0	95.3	94.3	93.5	93.5	93.3	18.3	16.5	14.8	14.9	14.3
GFY	96.4	62.0	1.3	0.0	0.0	98.5	97.0	95.2	94.9	94.2	13.4	6.8	5.7	5.4	5.0
GBY	93.5	33.6	1.7	0.0	0.0	97.9	96.3	95.9	95.7	94.7	20.9	16.5	14.7	15.4	12.5
DFX	90.3	10.9	0.0	0.0	0.0	99.9	98.8	98.4	98.5	97.9	N/A	N/A	N/A	N/A	N/A
DBX	87.2	31.8	0.0	0.0	0.0	99.9	96.9	94.6	94.2	94.5	N/A	N/A	N/A	N/A	N/A
DFZ	84.9	22.7	0.0	0.0	0.0	99.9	99.0	98.1	98.0	97.9	0.0	13.6	8.7	8.3	8.0

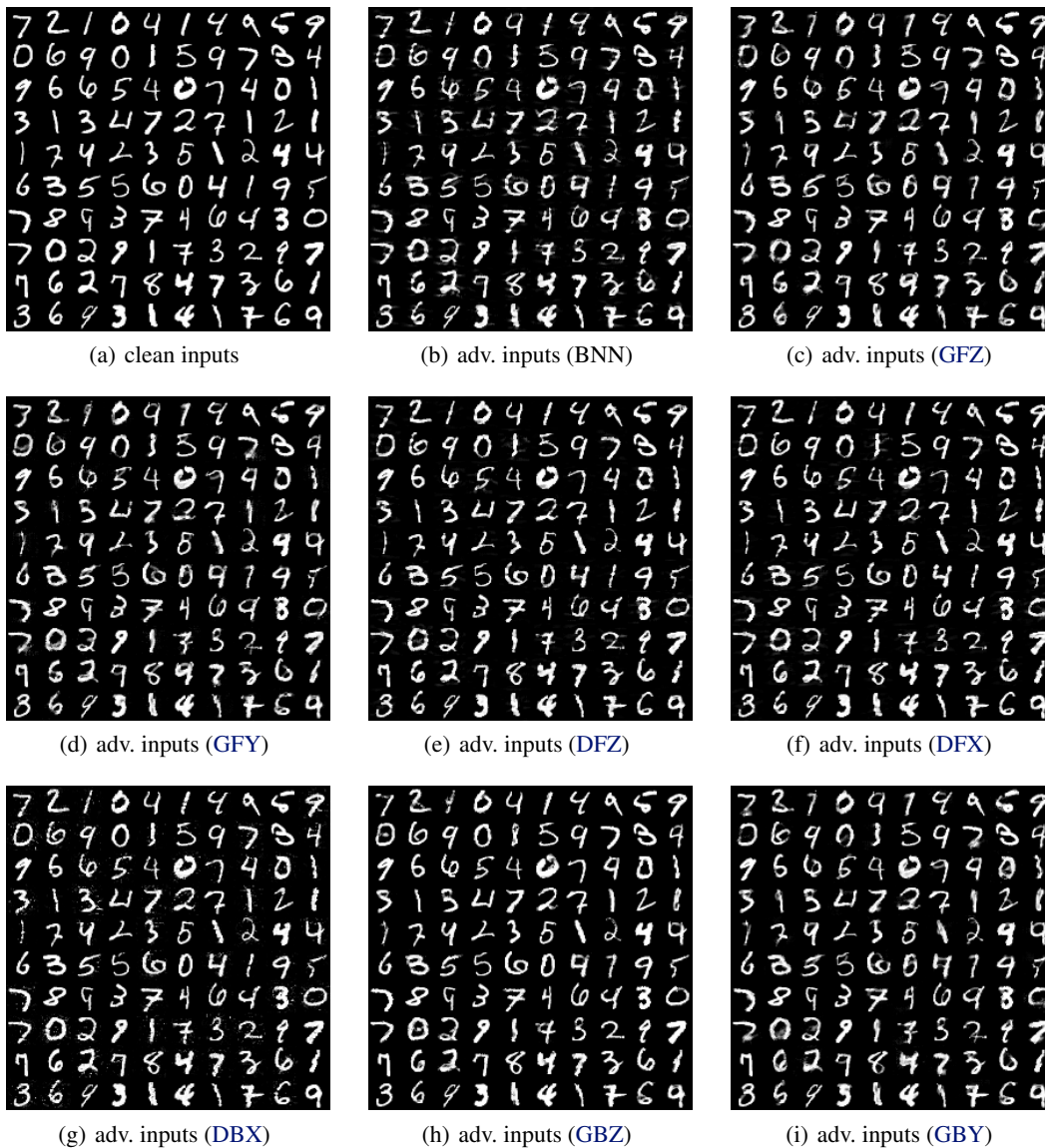


Figure E.1. Visualising the clean inputs of MNIST and the CW adversarial examples crafted on all the classifiers.

Table E.1. Clean test accuracy on CIFAR plane-vs-frog classification.

BNN	GFZ	GFY	DFZ	DFX	DBX	GBZ	GBY
97.00%	91.60%	91.20%	94.85%	95.65%	96.00%	89.35%	90.65

## E. Additional results

### E.1. White-box CW attack on MNIST

We visualise in Figure E.1 the crafted adversarial images using white-box CW attack.

### E.2. Clean test accuracy on CIFAR plane-vs-frog

We present in Table E.1 the clean accuracy on CIFAR plane-vs-frog test images (2000 in total).